FREE RADICAL REACTIONS

STUDIED BY FLASH PHOTOLYSIS

An investigation into the usefulness of a flash photolytic method of studying redox reactions of the benzyl radical

A Thesis submitted for the Final Honour School

Of Natural Science, Chemistry Part II

Brasenose College
Oxford

I. W. HUTCHINSON

June 1972

ACKNOWLEDGEMENT

The author would like to express his thanks to Professor Dainton for introducing him to this field of work, and to Dr. Pilling for his constant supervision and many helpful discussions throughout.

INDEX

CHAPTER 1 INTRODUCTION

1.1 Bimolecular Reactions in Solution

Several similarities and several striking differences are encountered in comparing reactions in the gas and liquid phases. The rate constant for a given reaction between free radicals and molecules is usually not greatly different in the two phases. However, certain thermal reactions of ions and photochemical primary processes involving ion formation and electron transfer become energetically far more favourable and are important in solutions of high dielectric constant. In the case of photochemical solution reactions, if homogeneous light absorption is maintained, the liquid phase systems are usually less complicated by wall reactions than are their gas phase counterparts because of much lower diffusion rates for liquid systems.

From a theoretical point of view, rates of reactions in solution have been satisfactorily interpreted in terms of both Collision and Transition State Theories. The uses and limitations of the former have been dealt with by Noyes[1] and North[2] and of the latter by North[2] and Benson[3].

Many reactions with an activation energy E_a, of about 10Kcal/mole are fast in the sense that special techniques are needed to measure their rates, but the temperature variation of the rate constant, k, is given by the usual Arrhenius Equation

$$k = A\, e^{(-\frac{E_a}{RT})}$$

in which the fraction of effective collisions, $e^{(-\frac{E_a}{RT})}$ is quite small. Such reactions may be called "activation-controlled" and taking the value of the pre-exponential factor, A, to be 10^{11} $M^{-1}s^{-1}$ (a value representative of many reactions between an ion and a molecule) bimolecular rate constants in the range $10^3 - 10^6$ $M^{-1}s^{-1}$ are found to be typical of such reactions.

For reactions that occur on practically every collision in the gas phase (*e.g.* free radical recombination and disproportionation, fluorescence quenching, and "allowed" energy transfer reactions), their rates in solution are frequently limited by the rate of diffusion of the reactants. Such "diffusion-controlled" reactions have apparent activation energies of 2-3 Kcal/mole and bimolecular rate constants in the region of $10^9 - 10^{11}$ $M^{-1}s^{-1}$, values which may be estimated from the modified Debye Equation[4,5]

$$k_{diff} = \frac{2RT}{3\eta}\left(2 + \frac{d_1}{d_2} + \frac{d_2}{d_1}\right) M^{-1}S^{-1}$$

$$= \frac{8RT}{3\eta} M^{-1}S^{-1}$$

$$\text{if } d_1 = d_2$$

where d_1, d_2 are the diameters of the reacting species (assumed spherical) and η is the viscosity of the solvent. Many refinements of this simple treatment have been made, giving better quantitative agreement with observed rate constants[1,6,7].

Perhaps the most striking of the effects encountered in solution phase reactions that is observed in the (dilute) gas phase is the "cage-effect"[8]. Free radical partners formed on homolytic bond rupture are encircled or "caged" by solvent molecules and, owing to slowness of diffusion in liquids, remain together for about 10^{-10} s, and this greatly increases the probability of mutual interaction. Two events now become possible:- (a) recombination to the parent molecule, which slows down the overall decomposition rate and (b) formation of new species e.g.

$$C_6H_5CH_2CO_2CH_2C_6H_5 \xrightarrow{h\upsilon} (C_6H_5CH_2)_2 + CO_2$$

which is unaffected by the presence of a scavenger. The theoretical aspects of this effect have been treated by several workers[1,9-14].

The particular case of free radical recombinations has been widely studied both in the gas phase[15-29] and in solution[28-44], and rate constants of the order of 10^{10} $M^{-1}s^{-1}$ are reported, showing such reactions to be diffusion-controlled processes. The radicals may be generated thermally (e.g. pyrolysis of acyl peroxides) or photochemically (e.g. from azo compounds) in a wide variety of solvents, and methods of monitoring the reaction are spectroscopic (ESR and UV) or by the rotating sector technique[42-44], and this has led to a large body of information concerning such reactions in solution.

1.2 Electron Transfer Reactions

In general, the mechanism of redox reactions may involve either (a) atom or group transfer or (b) electron transfer, both of which may occur by one of two mechanisms. Firstly, there is the "inner-sphere" mechanism[45-47]in which two metal ions are connected through a bridging ligand common to both co-ordination shells; and secondly, the "outer-sphere" mechanism[48-52]in which the inner co-ordination shells of both metal ions remain intact in the transition state.

Electron transfer reactions are well-characterized in the gas phase[53]. The situation in solution is more complex, and, from a quantum mechanical aspect, not even approximate calculations can be made because of the large numbers of particles to be considered. Two important restrictions are applicable to electron transfer processes in solution: firstly, rearrangement of co-ordinated groups cannot occur simultaneously with the transfer of the electron (a result of the Frank-Condon Principle) and, secondly, no overall change in electron spin can occur.

For many of these reactions it has been observed that $\Delta S^{\ddagger}$, the entropy of activation, is large and negative. Reorganization of the solvation spheres gives a positive contribution to $\Delta S^{\ddagger}$ since it involves partial "melting" of the solvent attached to its ions, and so there must be some larger negative term involved. This problem can be resolved by assuming an electron tunnelling mechanism for the electron transfer process in solution. The theory was initially developed by R.J.Marcus, Zwolinski, and Eyring[54,55] and utilizes Transition State Theory to derive an expression for the rate constant of the form

$$k = \mathrm{K}\frac{RT}{Nh}\exp\left(-\frac{\Delta \mathrm{G}^{\ddagger}}{RT}\right)$$

where K is the electron tunnelling transmission coefficient and $\Delta G^{\ddagger}$ the free energy of activation, includes the free energy of rearrangement and electrostatic repulsion terms. The theory then shows that the origin of the large negative value of $\Delta S^{\ddagger}$ is due to a contribution to $\Delta S^{\ddagger}$ of R ln. K by virtue of the tunnelling process, and since K is always less than 1, this will give the required negative term, the magnitude of which is calculated to be about 13e.u.[54]

The treatment of Marcus, Zwolinski and Eyring is based on a non-adiabatic process in that the electron jumps from one potential energy surface to another. R.A.Marcus[56], retaining the electron tunnelling hypothesis but now assuming an adiabatic process based on the idea of a single potential energy surface was then able to formulate a theory of electron transfer processes in solution. He assumed that the degree of spatial overlap of the orbitals of the reacting species in the activated complex is small and was able to show that the electron can transfer at distances considerably greater than that corresponding to the actual collision of the reactants *i.e*. it is related to the spatial extension of electronic orbitals. According to Marcus Theory, the rate constant for an electron transfer reaction may then be expressed in the form

$$K = Ze^{\{\frac{-W(R)+m^2\lambda}{RT}\}}$$

where Z is the collision frequency between two uncharged reactants in solution, W(R) is the coulombic work term involved in bringing the reactants together in the transition state, and m^2 λ is related to the work necessary to reorganize the co-ordination shell around the reactant ion. This theory, although quite useful, has been refined by Marcus and Hush[57-62] to give more accurate correlations with observed results.

1.3 The Use of Free Radicals in Electron Transfer Studies

Free radicals may take part in redox process of the type[63,64]

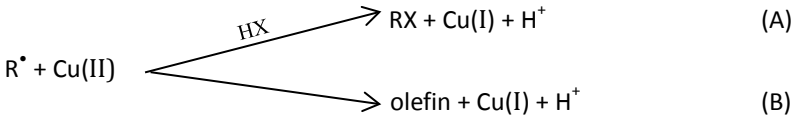

where HX = H_2O, HCl, CH_3COOH, and such reactions may be examined to determine any relationship existing between observed rates and thermodynamic properties of the metal species (*e.g*. redox potentials). Studies can be made in both aqueous and non-aqueous solutions, and particular advantages of the use in aqueous solutions are (a) otherwise-dominant coulombic interactions are minimized and (b) changes in pH or nature and concentration of other solutes affect only one reactant (both advantages being due to the absence of charge on the free radical).

Dainton *et al.*[65,66] have measured the combined rates of reactions (A) and (B) in the particular case where $R^{\bullet}$ is the growing radical chain in the polymerization of acrylamide and the metal ion is varied. A table containing some of their results is shown on p.8. These kinetic parameters are in better agreement with an electron-tunnelling mechanism than with an atom transfer process since they give rise to negative activation entropies[65].

Rate constants for the reaction between Cu(II) and simple alkyl radicals in aqueous acetic acid have been determined by Kochi and Subramanian[67] and typical values are shown on p.8.

Oxidation Of Polyacrilamide Radicals

Metal ion	Rate constant ($M^{-1}s^{-1}$)	E_a (Kcal $Mole^{-1}$)	A
Fe^{3+}aq.	2.8×10^3	2.35	1.45×10^5
	2.6×10^3	2.44	1.57×10^5
Cu^{2+}aq.	1.17×10^3	5.4	1.1×10^7
	1.4×10^3	5.3	1.0×10^7
Hg^{2+}aq.	1.05	6.2	4.2×10^4
Tl^{3+}aq.	0.34	2.5	
VO_2^{+}aq.	1.1×10^3		

Estimated Rate Constants for the Oxidation of Alkyl Radicals by Cu(II) at 57°C

Radical	E_a(Kcal $Mole^{-1}$)	Log A	Log k_{ox}
$C_2H_5^{\bullet}$	5.9	8.1	
n-$C_3H_7^{\bullet}$	6.7	8.3	7.64
$CH_3C^{\bullet}HCH_3$	6.3	8.3	7.70
n-$C_4H_9^{\bullet}$	5.4	7.9	8.05
$CH_3CH(CH_3)CH_2^{\bullet}$	6.5	8.7	7.70
$(CH_3)_3C^{\bullet}$	4.3	7.5	8.74
$CH_3CH_2C^{\bullet}HCH_3$	4.9	7.7	7.88

1.4 The Benzyl System

The benzyl radical ($C_6H_5CH_2^{\bullet}$ = $Bz^{\bullet}$) was first observed by Porter and Wright[68] in the flash photolysis of toluene, ethyl benzene, and benzyl chloride vapours, and subsequently in the solid[69] and liquid[70] phases. Details of the UV spectrum are shown in Figs. 1.1 and 1.2.

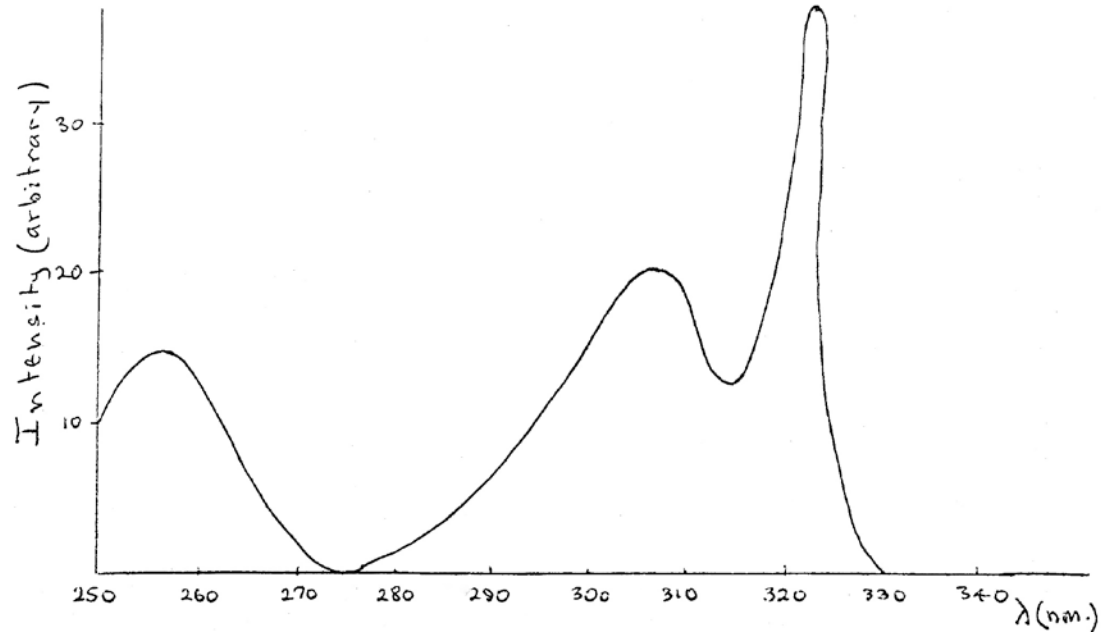

Fig. 1.1. Absorption Spectrum of $Bz^{\bullet}$ obtained by the flash photolysis of toluene[71]

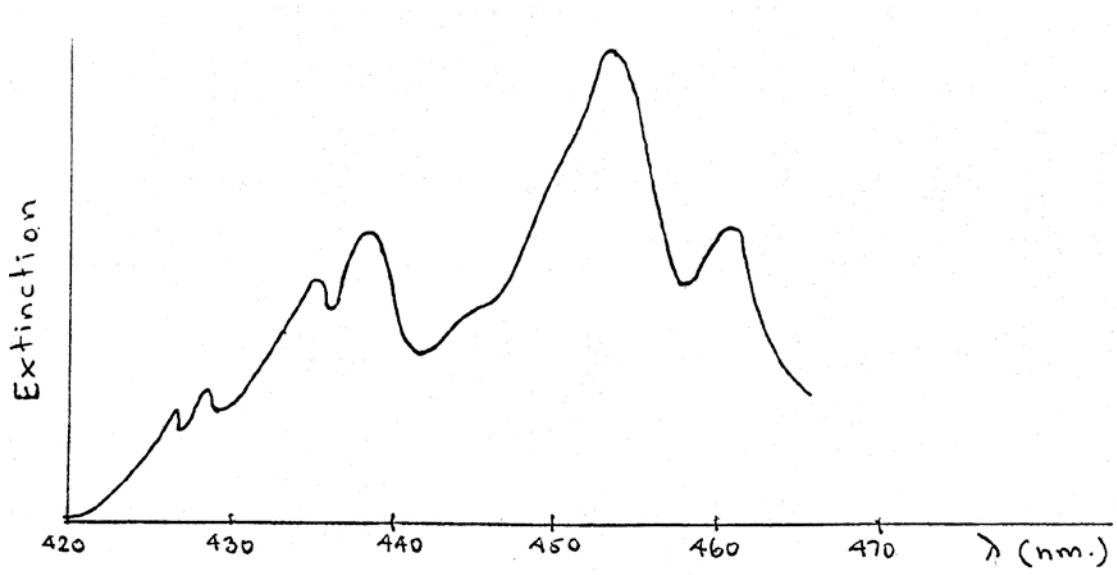

Fig. 1.2 Densitometer Traces of the $Bz^{\bullet}$ Spectrum. Obtained from 10^{-2}M. solutions of Toluene in 3-Methylpentane at 77°K using a 20 cm path length.[69]

Bands are found with peaks at 258nm, 307 and 318nm, and a weaker system whose most intense peak is at 452.7nm. These correspond to the transitions $3^2B_2 \longleftrightarrow 1^2B_2$[71], $2^2A_2 \longleftrightarrow 1^2B_2$[71], and $1^2A_2 \longleftrightarrow 1^2B_2$[72] respectively.

The peak at 318nm Is of highest intensity and is thus useful for monitoring reactions of the benzyl radical by a spectrographic method. However, widely divergent values of the extinction coefficient have been reported: 1.1 x 10^3[73], 1.9 x 10^4[74,75], and 1.2 x 10^4 $M^{-1}cm^{-1}$[41]. Higher values appear more

likely (since low values suggest a symmetry-forbidden transition) but involve several assumptions, and were also determined in low-temperature glasses.

Porter and Windsor[70] showed that the radical disappears in liquid paraffin by a diffusion-controlled reaction and suggested a bimolecular collision leading to dibenzyl. This was verified and the second-order rate constant evaluated in cyclohexane and benzene, giving values of 2-4 x 10^9 $M^{-1}s^{-1}$ [41,42,76].

1.5 Aims of present work

Several aims exist in the work undertaken here. The chief aim is to determine the usefulness of studying redox reactions involving free radicals (in particular the benzyl radical) by a flash photolytic procedure. The benzyl radical is particularly suited to studies of this kind utilizing the flash photolytic procedure (see Experimental section) since the strong absorption band at 318nm. Can be used to monitor concentration changes of the radical in a given reaction, and the radical has a relatively long half-life (of the order of milliseconds for micromolar initial concentrations of the radical) and is thus in the range of conventional flash photolysis systems. Rate constants for redox reactions between benzyl radicals and various metal species are then possibly opened to a quick and simple method of determination.

Using the photolysis of benzyl phenylacetate ($\phi CH_2CO_2CH_2\phi$) as a source of benzyl radicals, it should also be possible to undertake a study of the cage effect in various solvents (*e.g.* methanol/water, cyclohexane) since the analogous compound azotoluene ($\phi CH_2N_2CH_2\phi$) is known to undergo cage recombination of benzyl radicals to a very great extent[77]. A study of the temperature dependence of cage recombination versus non-cage recombination should be particularly easy using the flash photolysis technique.

CHAPTER 2 EXPERIMENTAL TECHNIQUES

2.1 The Flash Photolysis System

i) General Remarks

The flash photolysis apparatus is shown schematically in Figs. 2.1 and 2.2. A bank of ten 1μF rapid-discharge capacitors connected in parallel was charged to a high voltage (10-20Kv.) by means of a 100W 25KV D.C. power supply. They were then discharged through two quartz lamps by shorting the solenoid-activated switch, S. This produced a pulse of light which decayed to 1/e of its initial value in a time of *ca.* 25μs. (Fig. 2.3), and with total energy of 500-2000J. The lamps and reaction vessel were placed in a polished aluminium housing.

ii) Flash Lamps

The two flash lamps were constructed from high-purity quartz tubing. Electrodes were sealed into both ends of the tubing and the interior of the lamps washed in aqueous hydrogen fluoride solution to remove all adsorbed substances from the quartz surface. Each lamp was evacuated and heated to dull red heat, the whole system being kept under vacuum, until the entire length of the lamp had been heated. After cooling, the lamp was filled with krypton to a pressure of 6 Torr, and connected to the capacitor bank to be fired about fifty times at 10KV. The electrode connections were reversed and the lamp was fired another fifty times to ensure both electrodes were degassed to the same extent. The whole process from evacuation was then repeated. Finally, the lamps were filled with 6 Torr of krypton and sealed off.

Fig. 2.1 Physical Arrangement of Flash Photolysis System

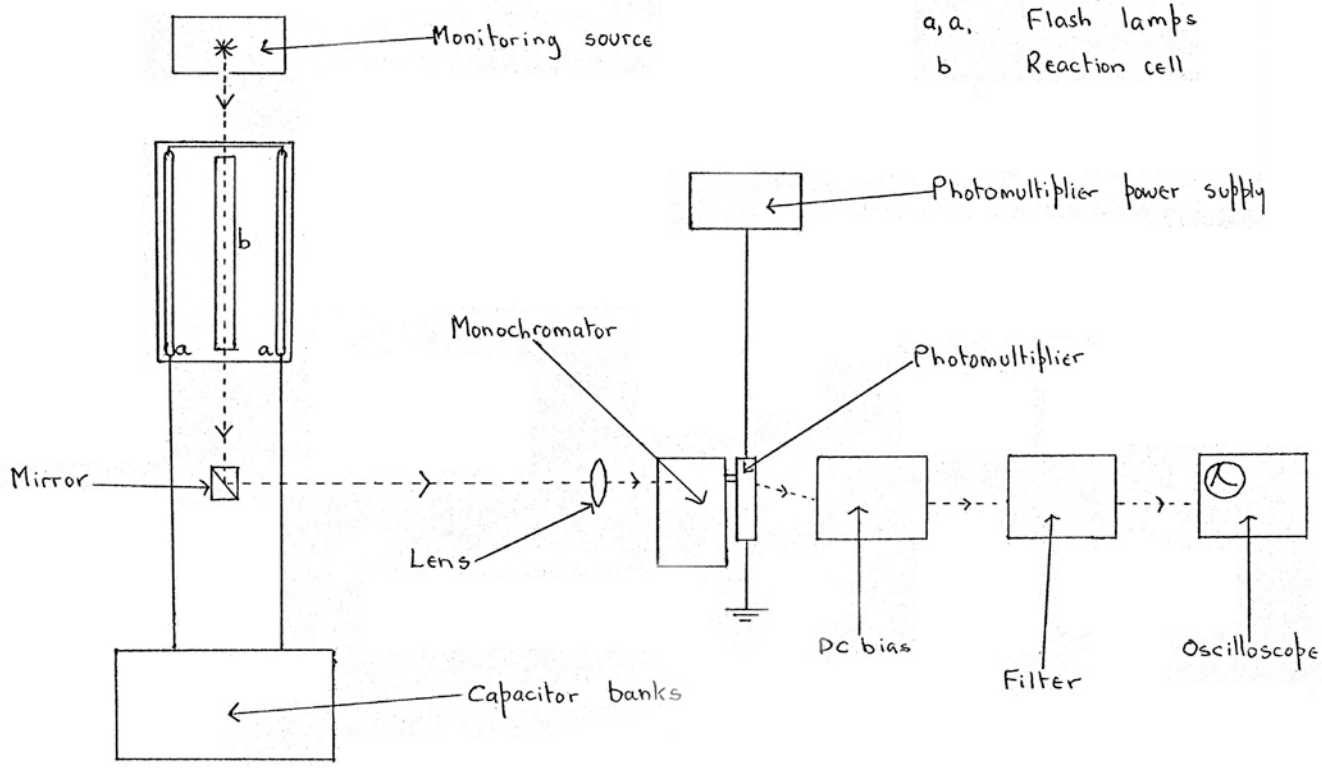

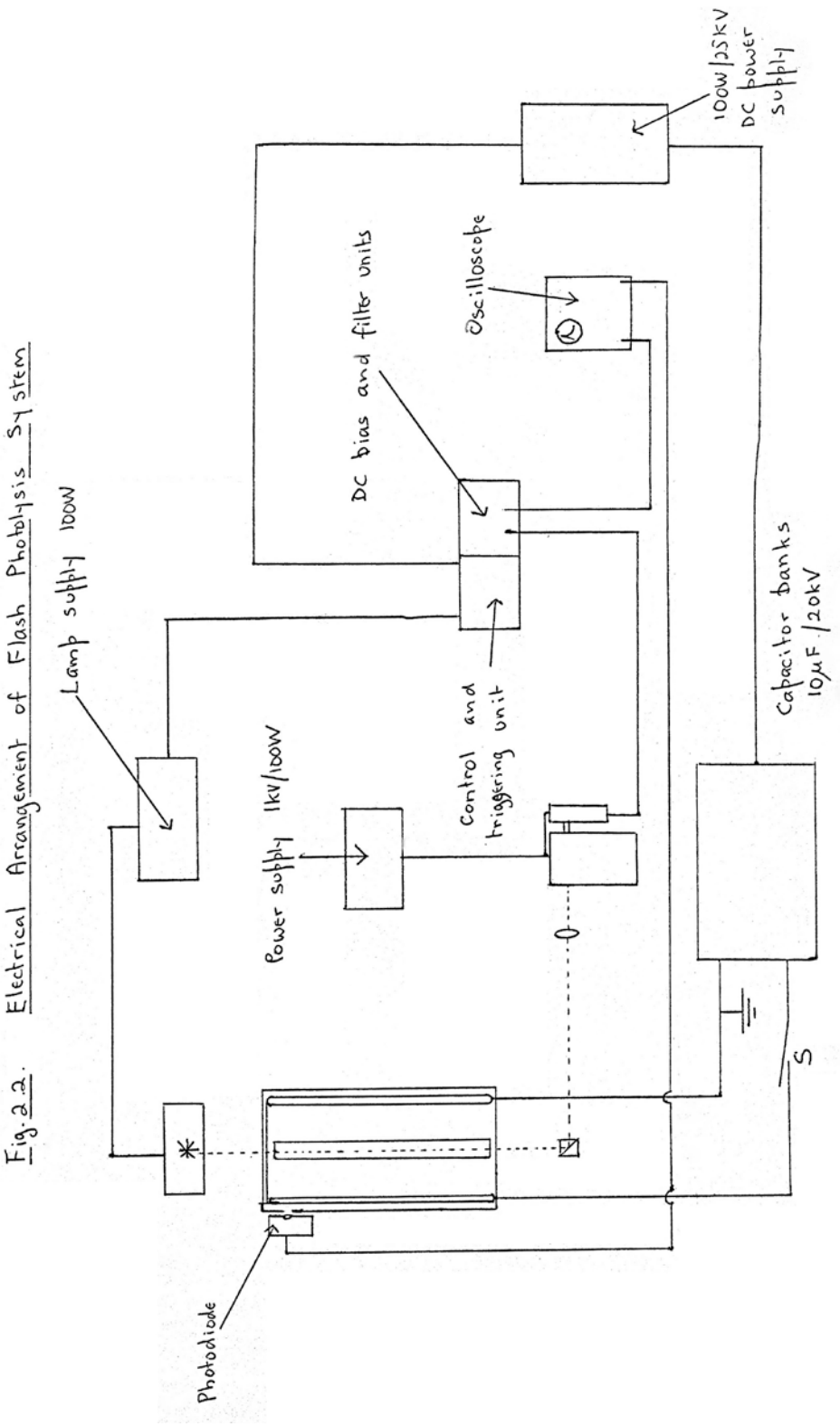
Fig. 2.2. Electrical Arrangement of Flash Photolysis System
Lamp supply 100W
Power supply 1kV/100W
Control and triggering unit
DC bias and filter units
Oscilloscope
100W/35KV DC power supply
Capacitor banks 10μF/20kV
S
Photodiode

Fig 2.3. Oscilloscope Trace of Photoflash

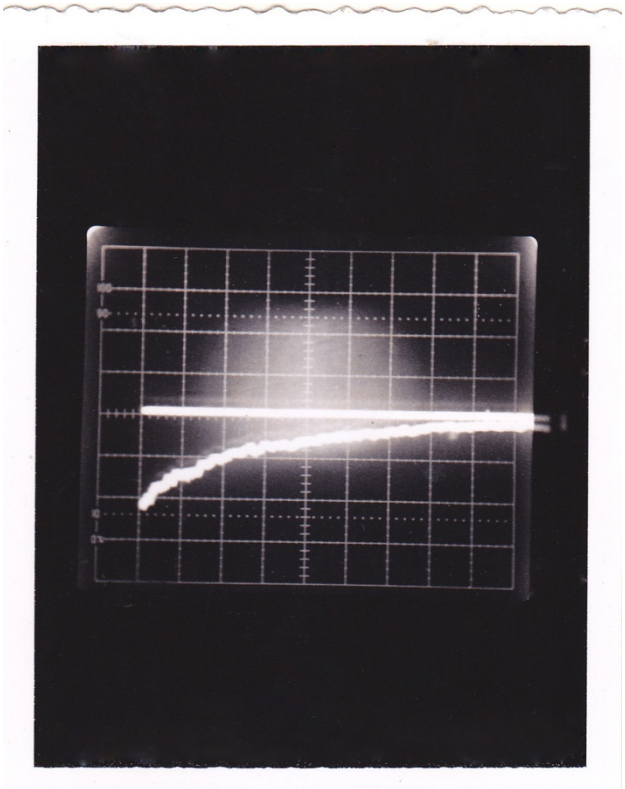

Wavelength	= 500nm
Vertical Sensitivity	= 50mV/div
Horizontal Sensitivity	= 10µs/div
Photoflash Energy	= 500J

iii) The Monitoring Source

The background source was a 100W quartz-iodine lamp operating at 12V. The wavelength characteristics of the source show maximum intensity at about 900nm, falling off rapidly in the near ultra-violet but with sufficient output in the region of the benzyl transition at 318nm for the purposes of this investigation.

iv) Optics

The monitoring beam leaving the reaction vessel was bent through an angle of 90^{o} with a plane silvered mirror. This horizontal beam was then focused on the slit of the monochromator by means of a quartz lens whose focal length was adapted to the aperture of the monochromator (*i.e.* with a focal length of about 20cm).

v) The Monochromator

The monitoring beam was dispersed by means of a Hilger and Watts D292 monochromator having a dispersion of 7nm/mm. This was calibrated against the known wavelengths of the emission lines from a low-pressure mercury lamp *viz.* the lines at 253.7, 296.7, 313, 334, 366, 405, and 426nm. The monochromator reading corresponding to each line (shown by maximum deflection on the oscilloscope) was compared with the true wavelength of the particular line and the correction plotted as a function of wavelength. The average correction to be applied to the monochromator reading is then the area enclosed by the graph divided by the wavelength spread of the measurements. Results are shown in Table 2.1.

Table 2.1 Corrections to Monochromator Reading

Monochromator Reading (nm)			**True (nm)**	**Correction (nm)**
Forwards	**Backwards**	**Average**		
251.5	252.5	252	253.7	+1.7
295	295.5	295.2_5	296.7	+1.5
311	311	311	313	+2.0
332.5	332.5	332.5	334	+1.5
363.5	363.5	363.5	366	+2.5
403	403	403	405	+2.0
434	434	434	436	+2.0

The alignment of the optical system is checked by passing the light beam from a 1mW Spectra Physics helium/neon laser through the monochromator in the reverse direction and then tracing its path back through each component to the centre of the monitoring lamp.

vi) The Photomultiplier

Dispersed light from the monochromator was passed to a side-windowed nine-stage S5 phototube (EMI 9660B) which was operated at 1KV from a Farnell E2 EHT unit. The last two dynode stages of the photomultiplier were shorted out to reduce the noise level. The output of the photomultiplier was adjusted, where possible, to 1V.

The photomultiplier response was determined by placing a series of filters of different optical densities in the light beam and monitoring the changes in output voltage as measured on the oscilloscope. The voltage was plotted as a function of the relative incident light intensity as shown in Fig. 2.4.

Fig. 2.4

Linearity of Photomultiplier Response

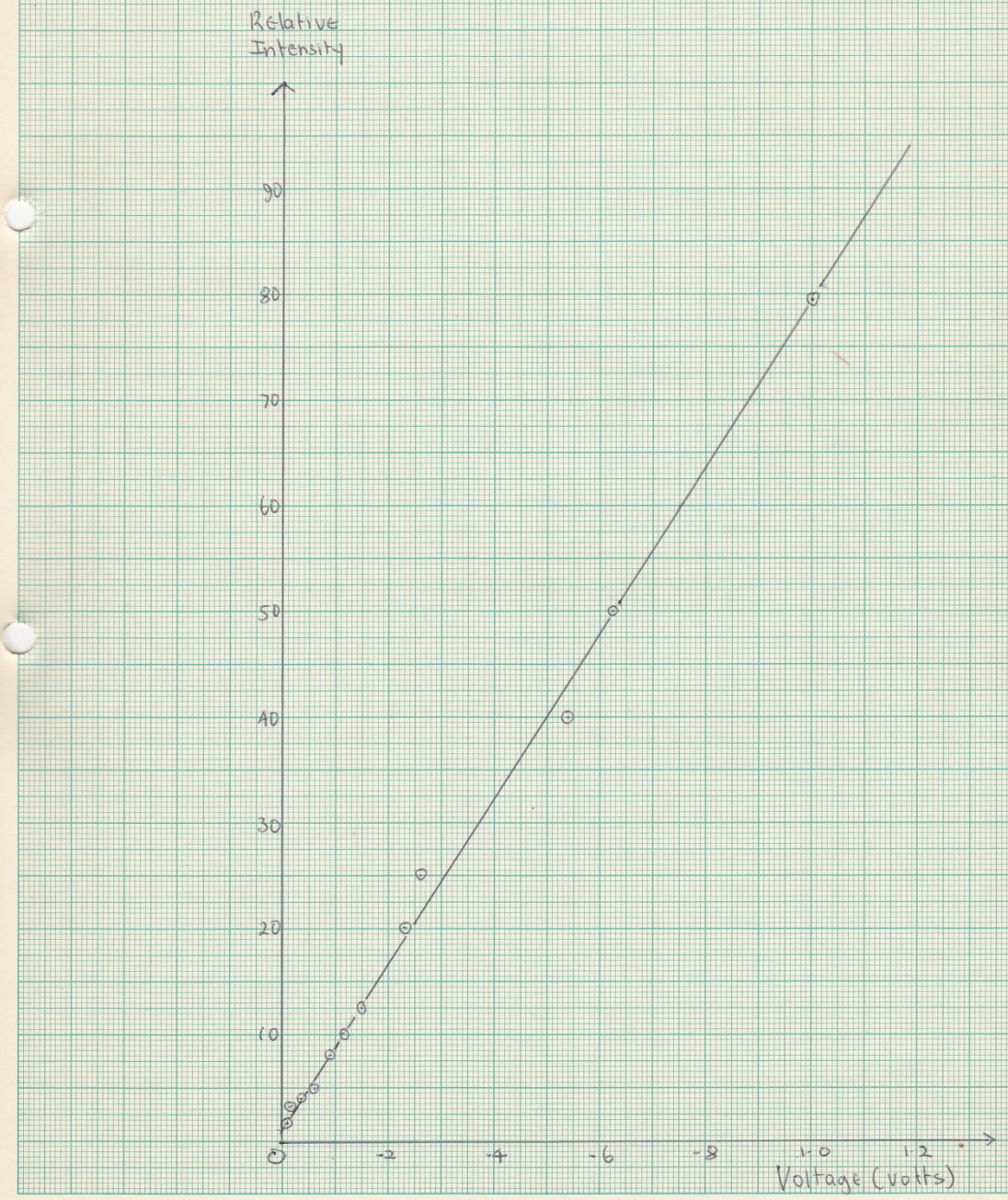

vii) DC Bias Unit

When measuring small absorptions it was desirable to operate the oscilloscope at high vertical sensitivities (<50 mV/div.). To achieve this, the total signal was offset using a DC bias unit consisting of a stabilized power supply and a potentiometer.

viii) The Filter Unit

High frequency noise from the quartz-iodine lamp was reduced by introducing π-type filters between the photomultiplier output and the oscilloscope input. By using various filters with varying cut-off frequencies it was possible to reduce the noise but still to obtain a faithful reproduction of the transient signal. Since most transients can be represented by low-frequency fundamentals (100KHz-100Hz) the filter unit can be designed to pass these frequencies unattenuated but to attenuate the high-frequency content. The time constant of the filter circuit was made at least five times less than the transient half-life for all decays.

ix) The Oscilloscope

The signal was then passed to an oscilloscope. Two types of oscilloscope were used – a Tektronix Type 453 and a Telequipment Type D53, both having a high sensitivity range (down to 5mV/div.). Light from the photoflash was allowed to fall on a photodiode and the output from this was used to externally trigger the oscilloscope. Traces were recorded on Polaroid film and then measured with an x-y travelling microscope.

x) Reaction Cells

The cylindrical reaction cells were constructed entirely of silica with dimensions 20cm x 1.6cm diameter. There was an outlet arm at each end of the cells to allow them to be filled with degassed solution.

2.2 Materials and Purifications

i) Cleansing Procedure

To minimize contamination by impurities all glassware used was subject to a strict cleansing procedure. Generally, this consisted of first washing with permanganic acid (concentrated sulphuric acid + potassium permanganate), rinsing, and then washing with a mixture of hydrogen peroxide and nitric acid. Further washing was with water of increasing *viz.* tap water, distilled water and, finally, triply-distilled water, the apparatus then being dried in an oven. Any water used as a solvent was also triply-distilled.

ii) Methanol

Purification of methanol was attempted by two methods. The first method consisted of heating 50cm^3 of Fisons AR grade methanol under reflux with 5g. of magnesium and 0.5g. of iodine until all reaction had ceased. The remainder of the methanol was added (usually about 500cm^3) and refluxed with a slow bleed of oxygen-free nitrogen for about 4 to 5 hours. The methanol was then distilled and the middle fraction of the distillate collected at a reflux ratio of 5:1.

Purification by the second method involved dissolving two lumps of sodium (cleaned under Fisons AR petroleum ether) and 7g. of BDH sodium borohydride in a winchester volume of AR methanol. The solution was refluxed for an hour in an atmosphere of oxygen-free nitrogen and distilled under the same conditions as the above method.

iii) Cyclohexane

The required volume of BDH AR cyclohexane was initially washed several times in a separating funnel with concentrated sulphuric acid until no further discolouration of the acid was observed. After further washing with distilled water the cyclohexane was allowed to dry overnight over anhydrous calcium chloride. The purification was then completed by refluxing the solvent for an hour in the presence of a few grams of sodium borohydride and an atmosphere of nitrogen, distilling and collecting the middle fraction of the distillate at a reflux ratio of 5:1.

iv) Benzyl Phenylacetate

Benzyl phenyl acetate (Emmanuel) was found (from Thin Layer Chromatography on a silica plate) to contain at least two impurities. Distillation was attempted as a means of purification but found to be unsatisfactory because the ester was extensively decomposed on heating, even under vacuum. It was therefore chromatographed on an alumina column using a mixture of petrol and ether (3:1) as elutant. A Thin Layer Chromatography test on several of the fractions showed that separation of the constituents was successful and the solvent was then removed with a rotary evaporator.

v) Degassing of Solutions

The solutions were thoroughly degassed to remove any dissolved oxygen by bubbling with nitrogen (BOC white spot) or argon (BOC). The apparatus used is shown in Fig. 2.5.

Initially, the whole system (minus the solution) was purged of air by opening taps A and C. The cell was then capped at the open end, the solution introduced and tap C closed and B opened. Degassing of the solution thus occurs and was allowed to continue for at least 30 minutes. Tap B was then closed and C opened, the cap was removed from the cell and the degassed solution was forced into the cell which was sealed off when full of solution.

Some solutions were degassed using the “freeze-pump-thaw” technique with the apparatus shown in Fig. 2.6. The solution was frozen in the dry ice/acetone bath and the whole vessel evacuated to remove any dissolved gas liberated. The tap was closed and the solution allowed to warm up again and the whole cycle repeated five or six times. Finally, the degassed solution was tipped into the cell which was then sealed off whilst still under vacuum.

Fig. 2.5. Apparatus For Solution Degassing by Bubbling

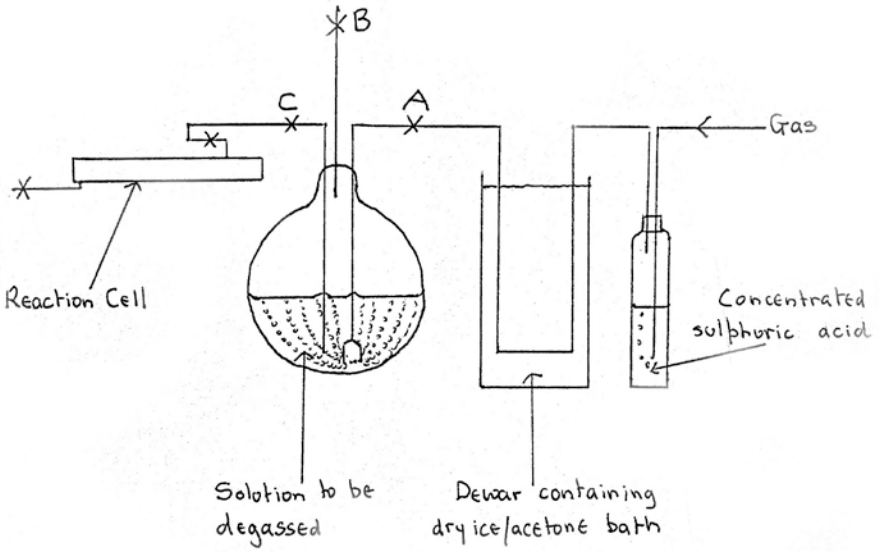

Fig. 2.6. Apparatus For Freeze-Pump-Thaw Degassing.

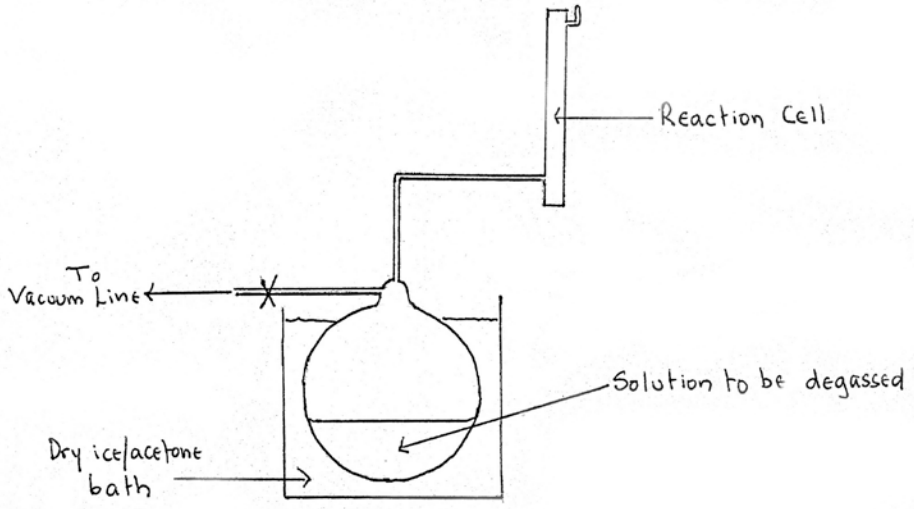

CHAPTER 3 RESULTS AND DISCUSSIONS

3.1 Characteristics of the System Used

i) Benzyl Phenylacetate

In order to produce a reasonable concentration of benzyl radicals, it is necessary that the compound chosen as the source should absorb a large amount of the high energy from the flash. Further, since the rate determinations depend on monitoring the absorption of the benzyl radical at 318nm, it is essential that the source of the radicals should not have a strong absorption band near this region. Benzyl phenylacetate was chosen as the source of benzyl radicals because of its simple photolysis to give two benzyl radicals and one molecule of carbon dioxide, and its absorption spectrum (recorded on an SP 700 spectrophotometer using a 0.5cm path length and a concentration of 2.5×10^{-4}M) is shown in Fig. 3.1. The spectrum shows a strong high-energy band at 215nm and no absorption at wavelengths greater than 280nm, thus confirming that benzyl phenylacetate is a suitable source.

ii) Absorbing Species at 318nm after Photolysis of Ester

The spectrum of the transient responsible for the absorption at 318nm was determined as a check on the photolysis of the benzyl phenylacetate. The peak optical density after flashing was measured over a range of wavelengths and the optical density plotted as a function of wavelength (Fig. 3.2.). A comparison with the known spectrum of the benzyl radical (Section 1.4) confirmed that the transient absorption was due to the benzyl radical.

Since the benzyl radical has a narrow absorption band and is known to decay by a second-order process, it was necessary to know the value of the effective extinction coefficient for any particular slit-width on the monochromator when checking the value of the second-order rate constant. The procedure used is described in Section 3.2.

3.2 Determination of Effective Extinction Coefficients at 318nm

After each photoflash, it was found that the intensity of transmitted 318nm light from the monitoring source had decreased (see Section 3.3.iii), and so to maintain a constant initial intensity of 1.0V for each decay it was necessary to increase the slit-width of the monochromator. Such a procedure resulted in an increased band-pass and a constant decrease in the effective extinction coefficient, ε, of the benzyl radical. Therefore the variation of ε with slit-width was determined.

The “infinitely-narrow” 313nm emission line from a low-pressure mercury lamp was used as the basis of the determination. A range of wavelengths around 313nm was scanned at several slit-widths and the intensity of the transmitted light measured on the oscilloscope. A graph of intensity against wavelength is shown in Fig. 3.3. Each of these traces was approximated to a triangle which was superimposed on the known spectrum of the benzyl radical as measured my McCarthy and McLachlan[73], taking the value of the extinction coefficient at 317.7nm to be 1.92×10^{4} $M^{-1}cm^{-1}$. The average extinction coefficient for each slit-width was then found by performing a series of summations of the products of area elements x extinction coefficients for each wavelength and dividing by the total area enclosed. A graph of mean extinction coefficient against slit-width is shown in Fig. 3.4.

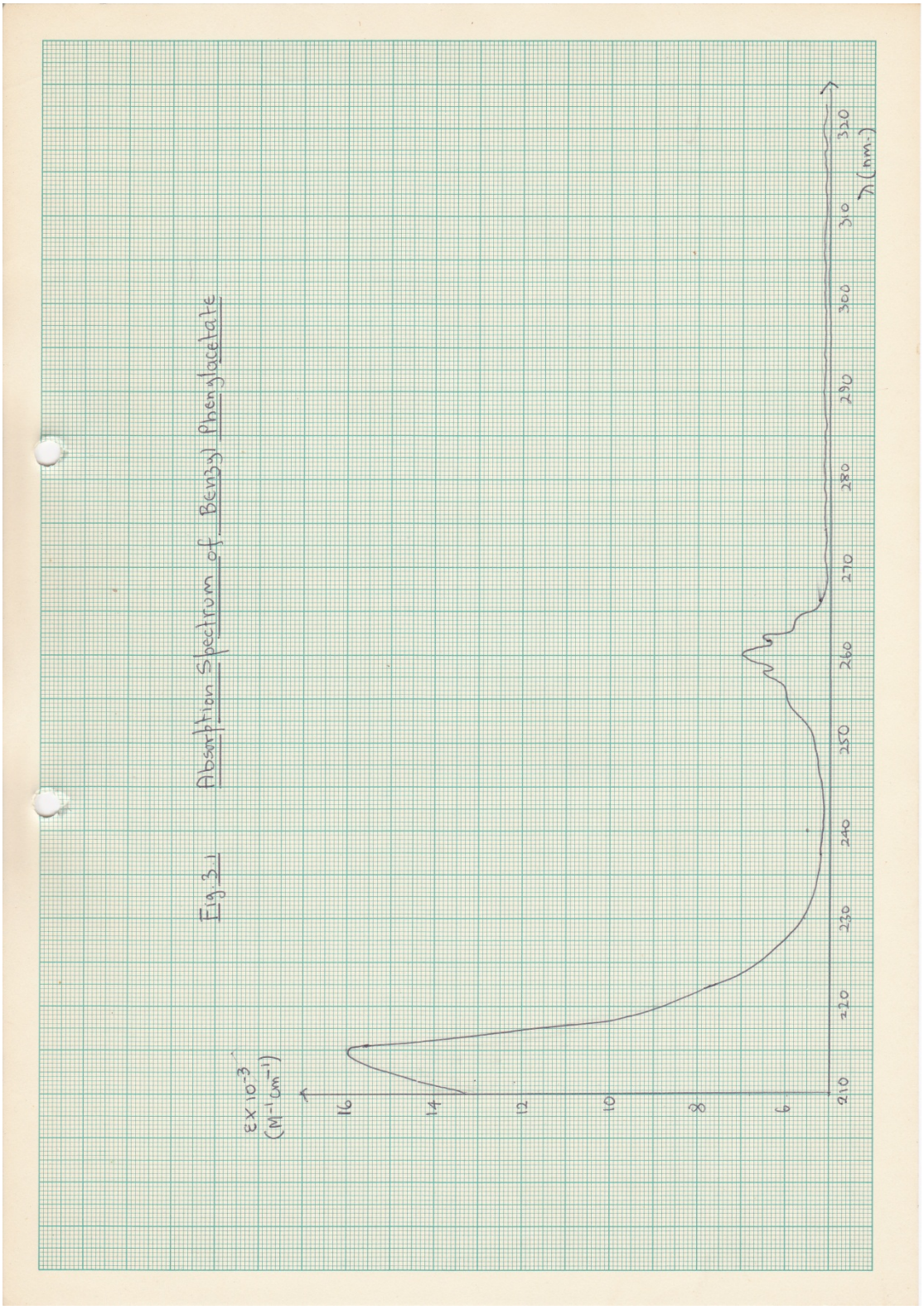
Fig 3.1 Absorption Spectrum of Benzyl Phenylacetate
ε x 10⁻³ (M⁻¹ cm⁻¹)
16
14
12
10
8
6
210
220
230
240
250
260
270
280
290
300
310
320
λ (nm)

Fig. 3.2 Spectrum of Species Absorbing at 318nm after photoflash

Fig 3.3 Determination of Band Pass for 313 nm Mercury Emission Line

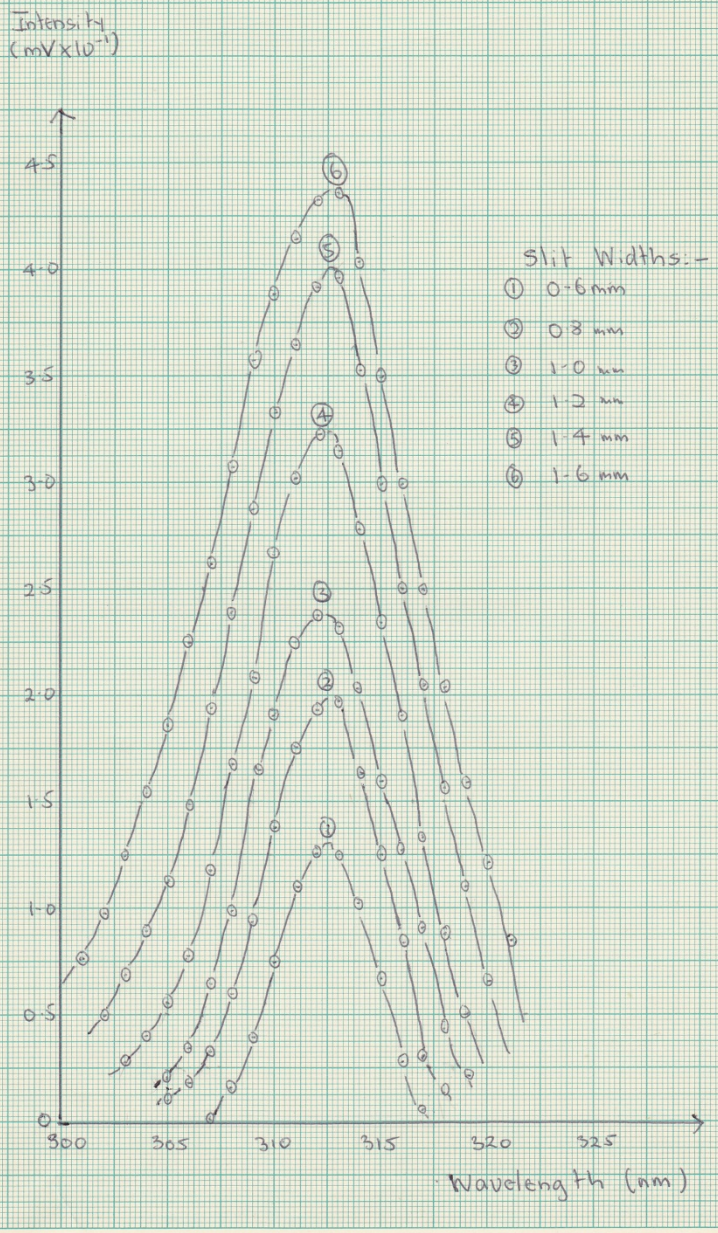

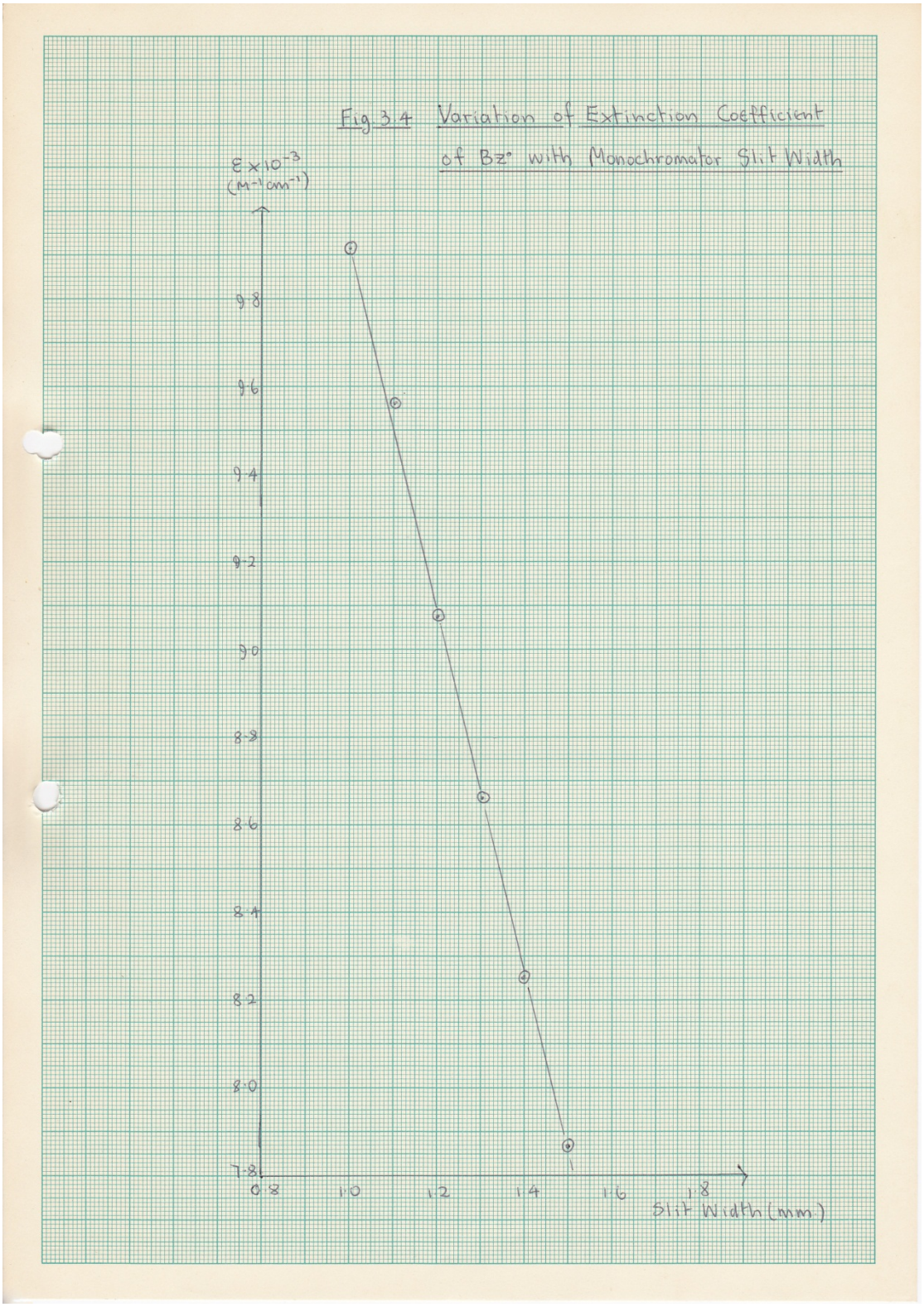
Fig 3.4 Variation of Extinction Coefficient of Bz° with Monochromator Slit Width
ε x 10⁻³ (M⁻¹cm⁻¹)
9·8
9·6
9·4
9·2
9·0
8·8
8·6
8·4
8·2
8·0
7·8
0·8
1·0
1·2
1·4
1·6
1·8
Slit Width (mm)

3.3 Transient Decays

i) General Observations

Benzyl phenylacetate was found to be insoluble in water but soluble in both methanol/water (5:1 v/v) mixtures and in cyclohexane. Solutions in both solvents were flash photolysed and a typical decay curve obtained is shown in Fig. 3.5.

The half-lives found for such decays were *ca.* 500µs and initial optical densities of the benzyl radical were in the range 0.01-0.05, giving initial radical concentrations ($[Bz]_{t=0}$) of between *ca.* 0.5-2.5 x $10^{-7}M^{-1}$. Assuming the literature values of k_2, the second-order rate constant (*i.e.* about 2 x $10^{9}M^{-1}s^{-1}$) such initial concentrations should lead to half-lives ($t_{1/2} = 1/k_2[Bz]_{t=0}$) of between 2 and 10ms. Such values are far greater than the observed half-lives and hence the assumption of a pure second-order decay must be invalid *i.e.* the kinetics show a composite first- and second-order decay rate.

ii) Effect of Reagent Purity

Initial rate determinations were carried out using AR grade materials which were not further purified. After purification by the methods described in Section 2.2, analysis of the decays showed no significant change in the value of the half-life, although estimates of the second-order component (expressed as k_2/ε) showed a decrease from (2.8 ± 0.3) x 10^{6} $cm^{+1}s^{-1}$ with AR materials to (0.73 ± 0.01) x 10^{6} $cm^{+1}s^{-1}$ with purified benzyl phenylacetate and methanol.

iii) Nature of Long-Lived Species

As Fig. 3.5 shows, photolysis of benzyl phenylacetate resulted in a permanent absorption by some long-lived photolysis product. This product was suspected to be dibenzyl and was characterized by measuring its UV absorption spectrum on the flash photolysis apparatus. The base-line was found by plotting the intensity of the transmitted light against wavelength over a wide range of wavelengths (230-450nm) before the solution of benzyl phenylacetate had been photolysed. The solution was then flashed ten times and new values of the light intensities were measured. From these measurements the percentage absorptions and optical densities of the product at various wavelengths were found. The spectrum thus obtained was compared to the known dibenzyl spectrum (Table 3.1 and Fig. 3.6) and was in good agreement (except at shorter wavelengths, which was possibly because of the low intensities of light from the quartz-iodine lamp and the consequent inevitability of larger errors).

Since dibenzyl has a high extinction coefficient at 318nm (1.8 x 10^{3} $M^{-1}cm^{-1}$) it was possible that the decay curves of the benzyl radical were being affected by the build-up of dibenzyl absorption to the maximum *i.e.* the observed absorption was due to both benzyl radicals and dibenzyl. The dibenzyl build-up would seriously affect the decay if it were built up over a relatively long period (about two half-lives). To check this, it was necessary to observe the dibenzyl build-up independently of the decay of the benzyl radical. This was possible by monitoring the photolysis at a wavelength where the extinction coefficient of dibenzyl was high and that of the benzyl radical low, and the region of maximum dibenzyl absorption (*ca.* 290nm) was convenient. Monitoring of the photolysis at 290nm showed that no appreciable build-up of dibenzyl occurred after the photoflash, suggesting that most of the dibenzyl was being formed by cage recombination of benzyl radicals (which cannot affect the observed decay curve) and so the only effect of the dibenzyl will be to displace the base-line of the decay (as in Fig. 3.5).

Fig. 3.5. Oscilloscope Trace of Benzyl Radical Decay

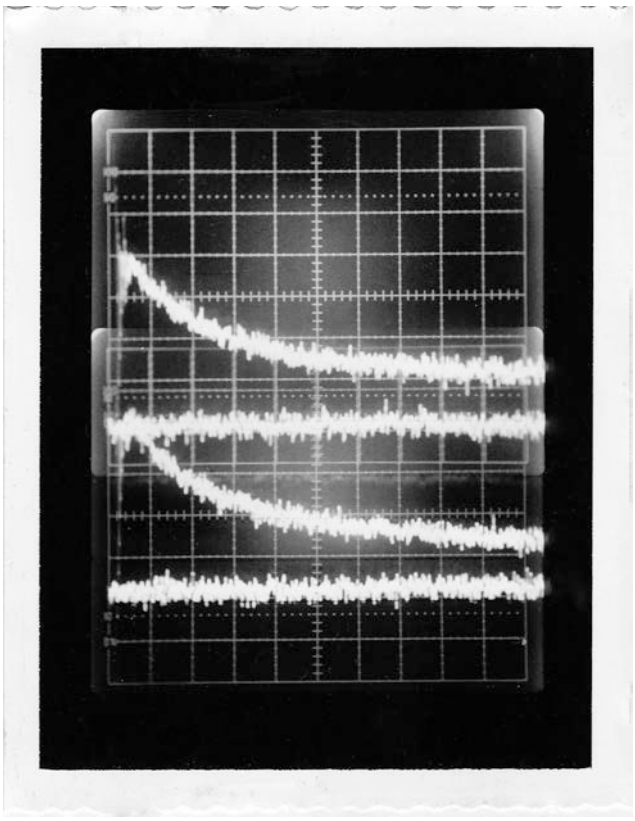

Wavelength	= 318nm
Vertical Sensitivity	= 20mV/div
Horizontal Sensitivity	= 500µs/div
Photoflash Energy	= 720J
Solvent	= Methanol/Water
Ester Molarity	= 1.5 x 10^{-3} M

Table 3.1 Absorption Spectrum of Long-lived Product

Wavelength (nm)	I_o (V)	I_{abs} (V)	Log ε *
230	0.012	0.00_5	3.55
240	0.01_3	0.00_6	3.37
250	0.01_4	0.00_5	3.28
260	0.01_5	0.00_4	3.10
270	0.02	0.00_6	3.22
280	0.06	0.03_5	3.50
290	0.21	0.16	3.63
300	0.36	0.20	3.50
310	0.67	0.34	3.40
320	1.00	0.38	3.20
330	0.09	0.00_8	2.38
340	0.15	0.09	1.17_5
350	0.23	0.10	1.15
360	0.33	0.10	1.04

* Values of O.D. rescaled to give log ε at 290nm = 3.63

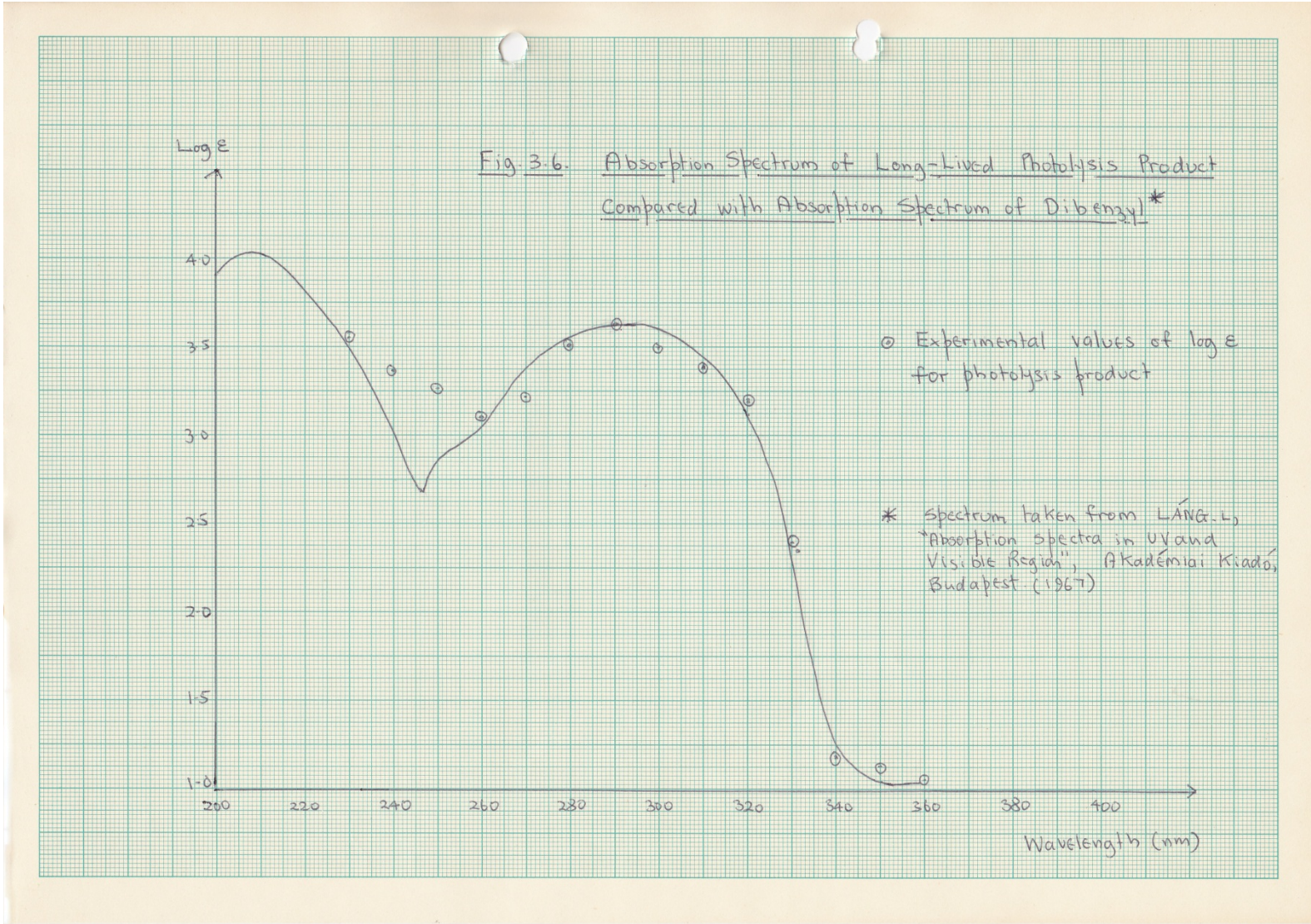

Fig 3.6. Absorption Spectrum of Long-Lived Photolysis Product Compared with Absorption Spectrum of Dibenzyl*

iv) Analysis of Decays

As expected on the basis of half-life estimates in Section 3.3.i, attempts to fit the decays to pure first- or second-order rate laws were not successful over the full time span of the measurements. Results were analysed for first-order decay by plotting –log(optical density) against time (since –log O.D. = $k_1t/2.303$ – log $O.D._{t=0}$) and for second-order decay by plotting (optical density)$^{-1}$ against time (since 1/O.D. = 1/$O.D._0$ + $k_2t/\varepsilon l$) and results for the decay of a 1.5 x 10^{-3} M solution of benzyl phenylacetate in methanol/water are given in Table 3.2 and Figs. 3.7, 3.8.

In general, it was found possible to obtain a reasonable straight line from the first-order plots if values at small times (when the second-order contribution is very large) were ignored. The value of k_1 obtained by this method could then be used to calculate a more accurate value for the second-order rate constant, according to the following analysis:

Rate of reaction with simultaneous first- and second-order decays is

$$-\frac{dc}{dt} = k_1\, c \;+\; k_2\, c^2$$

Or, since O.D. = εcl

$$-\frac{d}{dt}(O.D.) = \; k_1\,(O.D.) + \frac{k_2}{\varepsilon l}\;\;(O.D.)^2$$

Integrating from OD_0 at t = 0 to OD at time t gives

$$OD^{-1} = \left(\frac{k_1\,\varepsilon l + k_2 OD_0}{k_1\,\varepsilon l\, OD_0}\right)^{e^{k_1 t}} - \;\frac{k_2}{k_1 \varepsilon l}$$

and hence a plot of OD^{-1} against exp(k_1t) should have a negative intercept whose numerical value is equal to $k_2/k_1\,\varepsilon l$ from which the previously determined value of k_1 can be used to give a value for k_2/ε. A plot of this kind for the decay detailed in Table 3.2 is shown in Fig. 3.9, and similar analyses of other decays in both methanol/water and cyclohexane give values for the rate constants as

$$k_1 \;=\; (0.78 \;\pm\; 0.06)\text{ x } 10^3\ s^{-1}$$

$$\frac{k2}{\varepsilon} = \;(1.44 \;\pm\; 0.1)\text{ x } 10^5\ cm^{+1}s^{-1}$$

For typical slit-widths used in these determinations, the value of the effective extinction coefficient was about 0.95 to 1.1 x 10^4 M^{-1}cm-1, which gives an upper limit to k_2 of about 1,58 x 10^9 $M^{-1}s^{-1}$ which is on the low side of the literature values (*ca.* 2.0 x $10^9 M^{-1}s^{-1}$).

v) Lower Limit of Benzyl Extinction Coefficient at 318nm

The amount of dibenzyl produced by each benzyl decay can be easily found by the equation

O.D. (dibenzyl) = εcl

since all quantities are known or measured except the concentration. Assuming the only benzyl radicals produced are those seen in the decay curve, the concentration of benzyl radicals produced is twice the concentration of dibenzyl formed. Hence, knowing the initial optical density of the benzyl radicals, a value for the extinction coefficient of the benzyl radical at 318nm can be found. However, since the main dibenzyl production is probably by cage recombination of benzyl radicals, the concentration of benzyl calculated will be too high, and so such an estimation gives a lower limit for the value of the extinction coefficient. Estimations by this method tended to give results varying between 3700 and 5700 $M^{-1}cm^{-1}$, although the majority of the calculations suggested a limiting value of (4.6 ± 0.3) x 10^3 $M^{-1}cm^{-1}$.

vi) Flash Photolysis of Dibenzyl

Since dibenzyl has been shown to be formed as the permanent product after photolysis, it was necessary to determine whether subsequent flashing of the solution gave decays complicated by photolysis or electronic excitation of the dibenzyl. As a check on this, a 10^{-4} M solution of dibenzyl was flashed in both methanol/water and cyclohexane, but no transient absorption was observed in the region of 318nm, even at maximum vertical sensitivity on the oscilloscope.

Table 3.2 Analysis of Benzyl Decay in Methanol/Water

Time (ms)	Voltage (mv)	O.D. (x 10^{-4})	1/OD	-log(OD)	$e^{k_1 t}$
0.0	79.89	362	27.62	1.44	2.25
0.1	71.37	322	31.1	1.49	2.42
0.2	65.34	294	34.0	1.53	2.61
0.3	59.45	266	37.5	1.57	2.81
0.4	54.55	244	41.0	1.61	3.02
0.5	49.29	220	45.5	1.65	3.25
0.6	44.61	198	50.5	1.70	3.50
0.7	40.69	181	55.2	1.74	3.76
0.8	38.57	171	58.5	1.76	4.05
0.9	35.58	157	63.7	1.80	4.36
1.0	33.20	146	68.5	1.83^5	
1.1	31.52	139	71.9	1.85	
1.2	29.40	129	77.5	1.89	
1.3	27.31	120	83.3	1.92	
1.4	25.45	111	89.7	1.95	
1.5	23.95	105	94.8	1.97	
1.6	22.41	98	102.0	2.01	
1.7	21.10	93	107.5	2.03	
1.8	19.38	85	117.6	2.07	
1.9	17.88	79	126.6	2.10	
2.0	16.56	72	138.9	2.14	

Fig. 3.7 First Order Decay Plot for Benzyl Radical

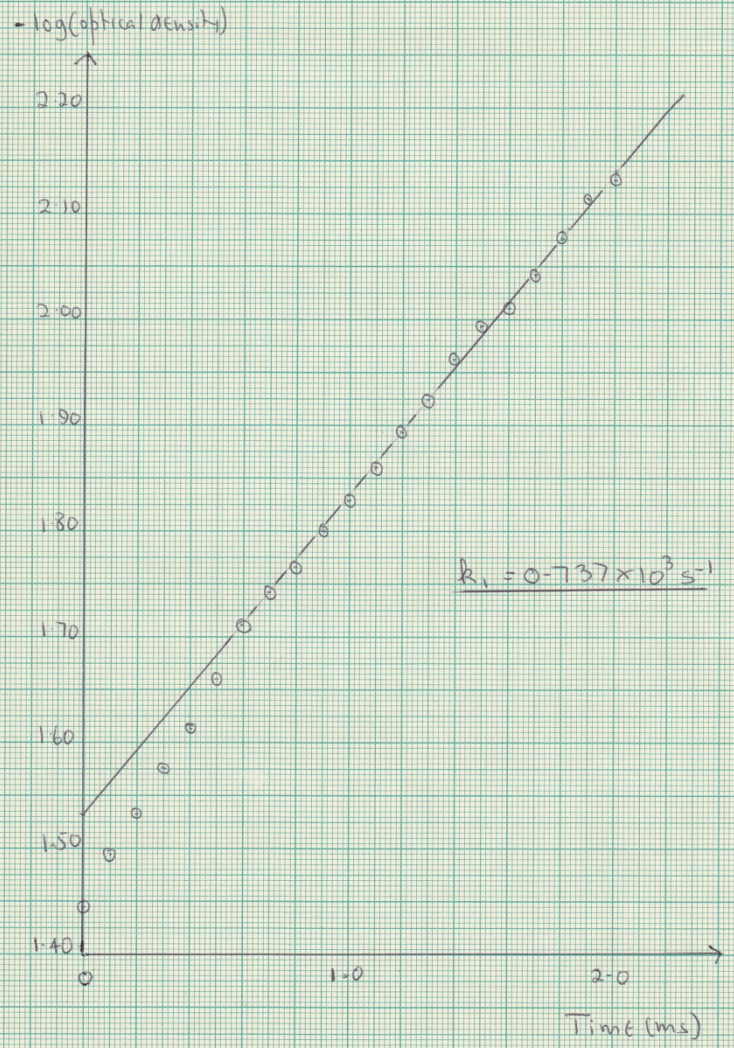

Fig. 3.8 Second Order Decay Plot for Benzyl Radical

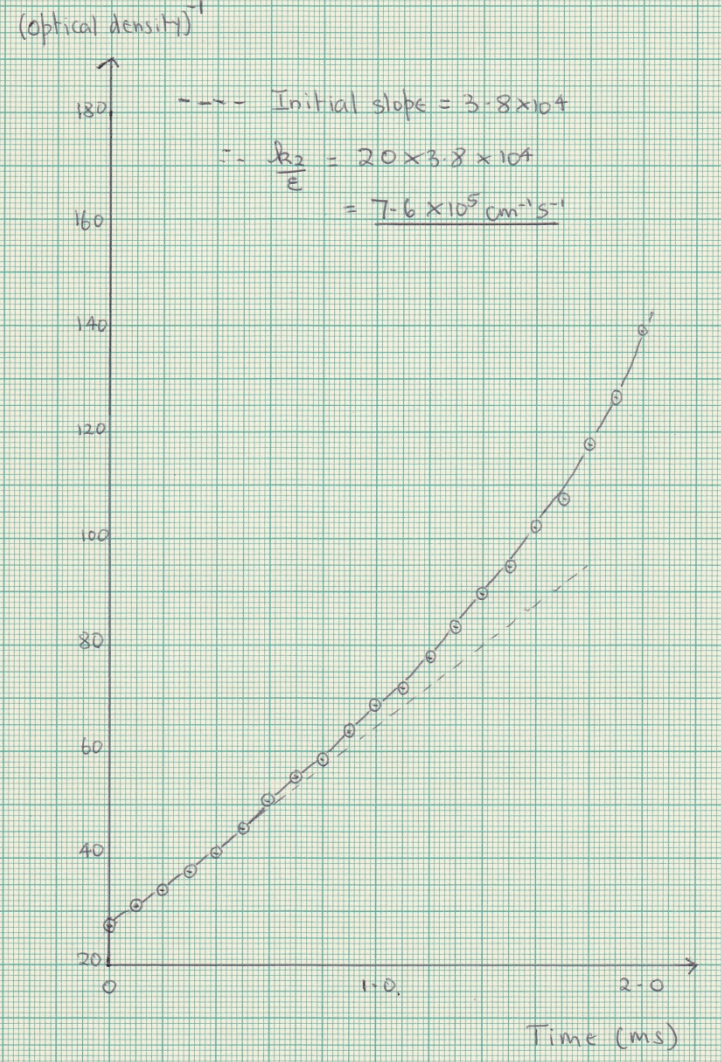

Fig. 3.9 Simultaneous First and Second Order Decay Plot for Benzyl Radical

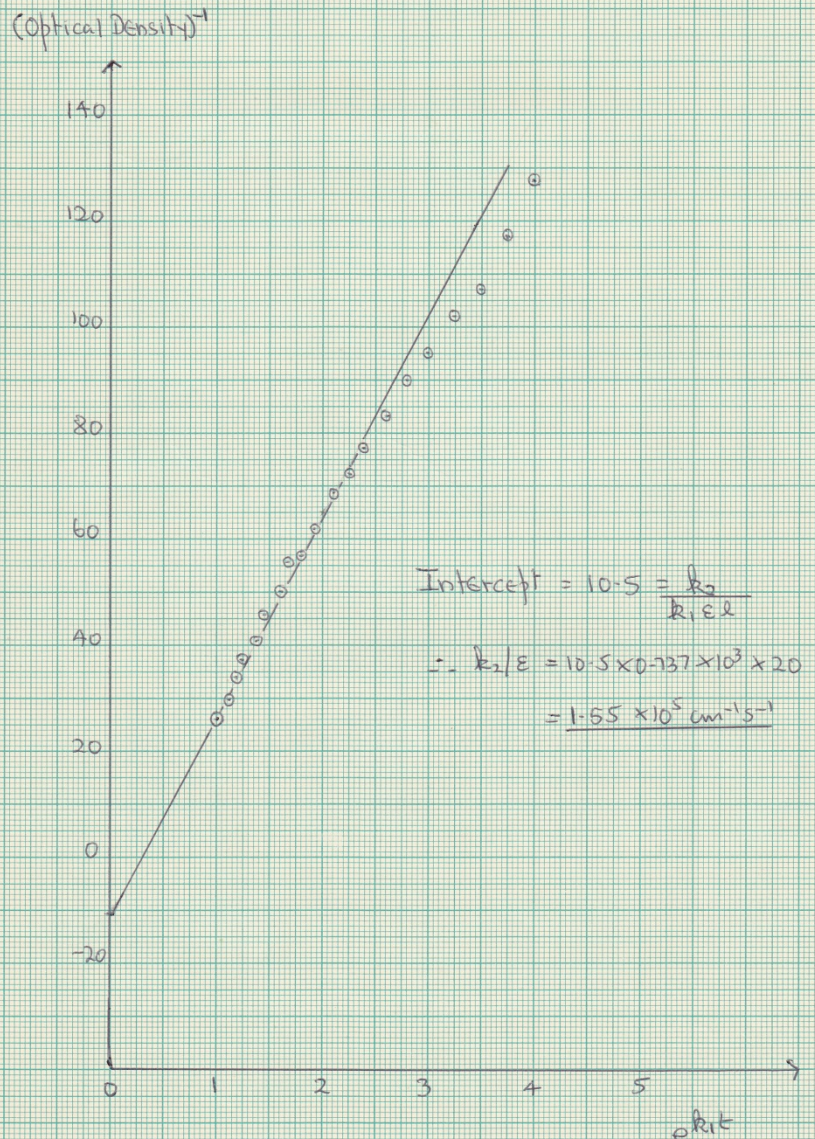

$$\text{Intercept} = 10.5 = \frac{k_2}{k_1 \varepsilon l}$$

$$\therefore k_2/\varepsilon = 10.5 \times 0.737 \times 10^3 \times 20$$

$$= 1.55 \times 10^5 \text{ cm}^{-1}\text{s}^{-1}$$

3.4 Redox Studies

i) Choice of Solute

Choice of metal species as oxidant for the benzyl radical was limited by two factors. Firstly, the species had to be those which were known to participate easily in redox reactions with free radicals, and initial possibilities were cupric salts ($CuSO_4$, $Cu(OAc)_2$, $Cu(ClO_4)_2$), ferric salts ($FeCl_3$, $Fe(CN)_6^{3-}$, $FeCl_4^-$, $FeBr^{2+}$) and, as a possible alternative to metal compounds, certain organosulphur compounds such as mercaptans and ethyl thioglycolate. The second requirement was that the species used should have no strong absorption bands near the 318nm region used to monitor the reactions, and this proved to be a serious limitation for all the above compounds except those of Cu(II). Ease of solubility was a possible criterion for the choice of oxidant, but no solubility problems were encountered in the case of the Cu(II) compounds mentioned in the concentration range used (*ca.* 10^{-4}M).

ii) Analysis of Decays

Each of the metal salts cupric acetate, cupric perchlorate, and cupric sulphate were used in attempts to find pseudo-first-order rate constants for the (schematic) redox reaction

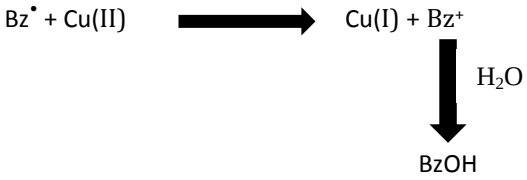

and some decay curves obtained are shown in Fig. 3.10 for the case of a 2.49 x 10^{-4}M cupric sulphate solution in methanol/water. Typical results obtained for each of the cupric salts are given in Tables 3.3, 3.4, and 3.5, and Figs. 3.11, 3.12, and 3.13.

From a theoretical point of view, assuming that the redox reaction is proceeding via pseudo-first-order kinetics, the rate constants obtained should be directly proportional to the concentration of cupric ion. However, the results obtained indicated that, in spite of the variation in cupric concentration, the value of the first-order rate constant was effectively the same in all cases, and, also, the half-life increased to about 900µs. Such results seem to indicate that the reaction being followed was not the straightforward redox reaction expected.

iii) Determination of the Nature of the Reaction with Cu(II)

Either of two possibilities for the process occurring in the presence of the cupric ion seems feasible. The first possibility is that some complex may be formed between Cu(II) and benzyl phenylacetate, and the observed photolysis may be that of this complex. To ascertain whether this was likely, absorption spectra were recorded on an SP 700 spectrophotometer for the ester alone and for the ester in the presence of cupric ion before and after several flashes (Figs. 3.14, 3.15). No change in the spectra were noted, making complex formation before photolysis appear unlikely.

The second possibility is that complex formation between the benzyl radical and the cupric ion occurs very rapidly after the photolysis of the ester and that the observed decay is a consequence of this complex breaking up. This possibility was tested by obtaining the spectrum of the absorbing species (as in Section 3.1.ii) and comparing it to the spectrum of the benzyl radical obtained by flashing the ester alone (Fig. 3.16). As the spectra show, it is impossible to draw a firm conclusion on this evidence alone about any difference in the nature of the absorbing species in each case.

Fig. 3.10. Oscilloscope Trace of Benzyl Decay in Presence of Cu(II)

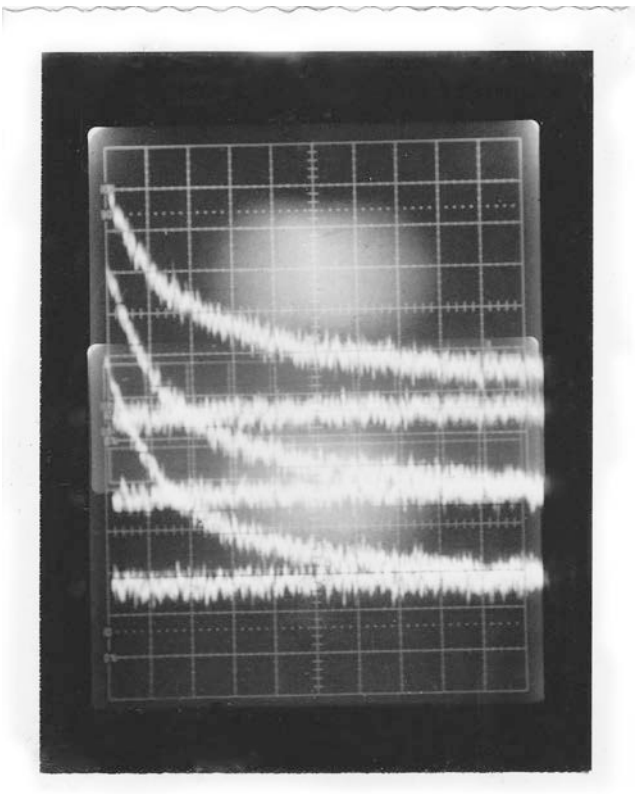

Wavelength	= 318nm
Vertical Sensitivity	= 20mV/div
Horizontal Sensitivity	= 500μs/div
Photoflash Energy	= 500J
Solvent	= Methanol/Water
Ester Molarity	= 1.5×10^{-3} M
Cupric Ion Molarity	= 2.49×10^{-4} M

Table 3.3 Benzyl Decay in Presence of $Cu(OAc)_2$

Time (ms)	Voltage (mV)	O.D (x 10^{-4})	-log(O.D.)
0.0	36.20	160	1.79
0.2	35.94	159	1.60
0.4	33.78	149	1.83
0.6	31.01	137	1.86
0.8	28.45	125	1.90
1.0	26.73	115	1.94
1.2	25.41	111	1.95
1.4	23.40	193	1.99
1.6	21.24	82	2.03
1.8	18.68	73	2.08
2.0	16.85	66	2.14
2.2	14.51	660	2.18

Table 3.4 Benzyl Decay in Presence of $CuSO_4$

Time (ms)	Voltage (mV)	O.D. (x 10^{-4})	-log(O.D.)
0.0	37.92	168	1.77
0.2	35.43	156	1.80
0.4	33.78	150	1.82
0.6	32.25	142	1.85
0.8	30.05	132	1.88
1.0	27.57	121	1.92
1.2	26.18	115	1.94
1.4	23.47	104	1.98
1.6	22.08	97	2.01
1.8	20.37	89	2.05
2.0	18.54	81	2.09

Table 3.5 Benzyl Decay in Presence of $Cu(ClO_4)$

Time (ms)	Voltage (mV)	O.D (x 10^{-4})	-log(O.D.)
0.0	88.88	405	1.39
0.2	74.33	336	1.47
0.4	60.77	272	1.56_5
0.6	48.56	216	1.70_5
0.8	44.28	196	1.78
1.0	37.70	167	1.84
1.2	32.80	145	1.88
1.4	29.80	131	1.92
1.6	27.42	120	1.96_5
1.8	24.57	108	2.01
2.0	21.90	97	2.04
2.2	20.66	90	2.08_5
2.4	18.94	82	2.13
2.6	16.89	74	2.17
2.8	15.43	67	2.19
3.0	14.70	65	2.23_5
3.2	13.35	58	2.27_5
3.4	12.21	53	2.30_5
3.6	11.44	49	2.33

Fig. 3.11 First Order Decay Plot for a 1.5×10^{-3} M Ester + 4.01×10^{-5} M $Cu(OAc)_2$ solution in Methanol / Water

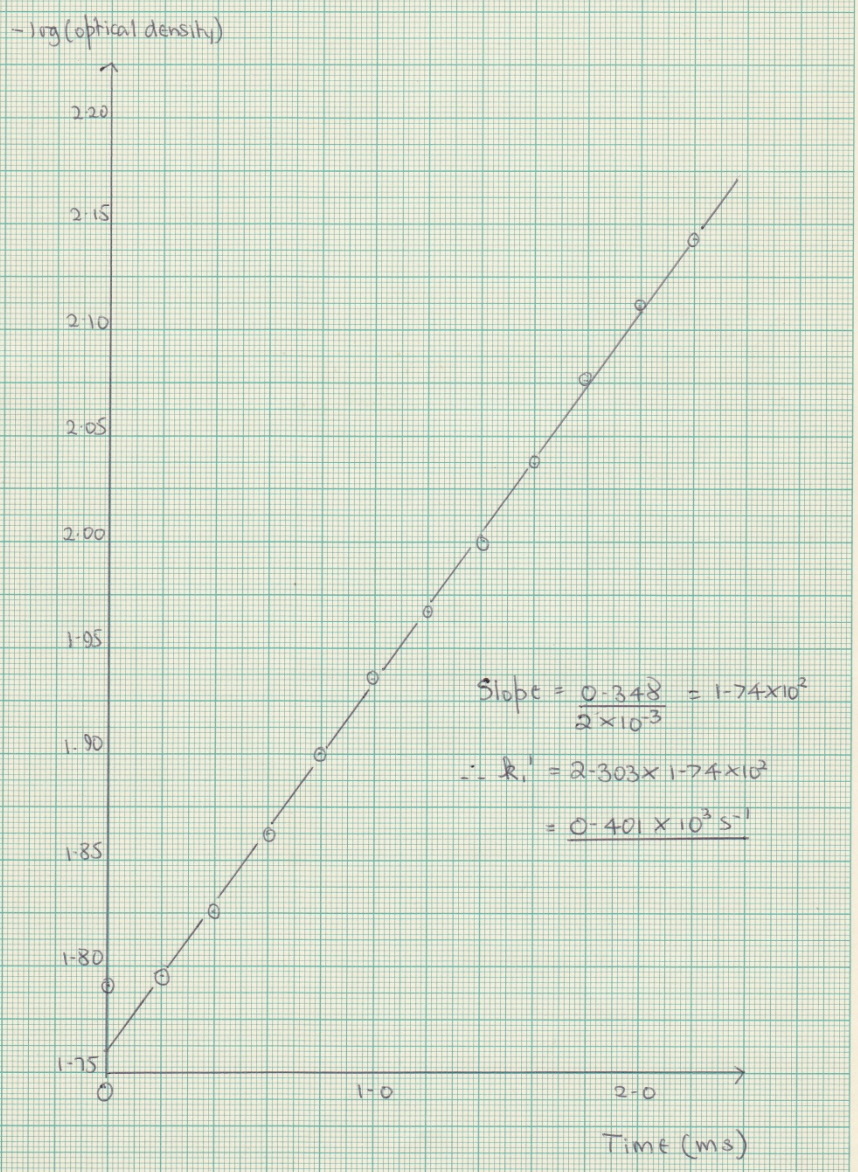

$$\text{Slope} = \frac{0.348}{2 \times 10^{-3}} = 1.74 \times 10^{2}$$

$$\therefore k_1' = 2.303 \times 1.74 \times 10^{2}$$

$$= \underline{0.401 \times 10^{3}\ s^{-1}}$$

Fig. 3.12 First Order Decay Plot for a 1.5×10^{-3} M Ester + 1.09×10^{-4} M $Cu(ClO_4)_2$ solution in Methanol | water

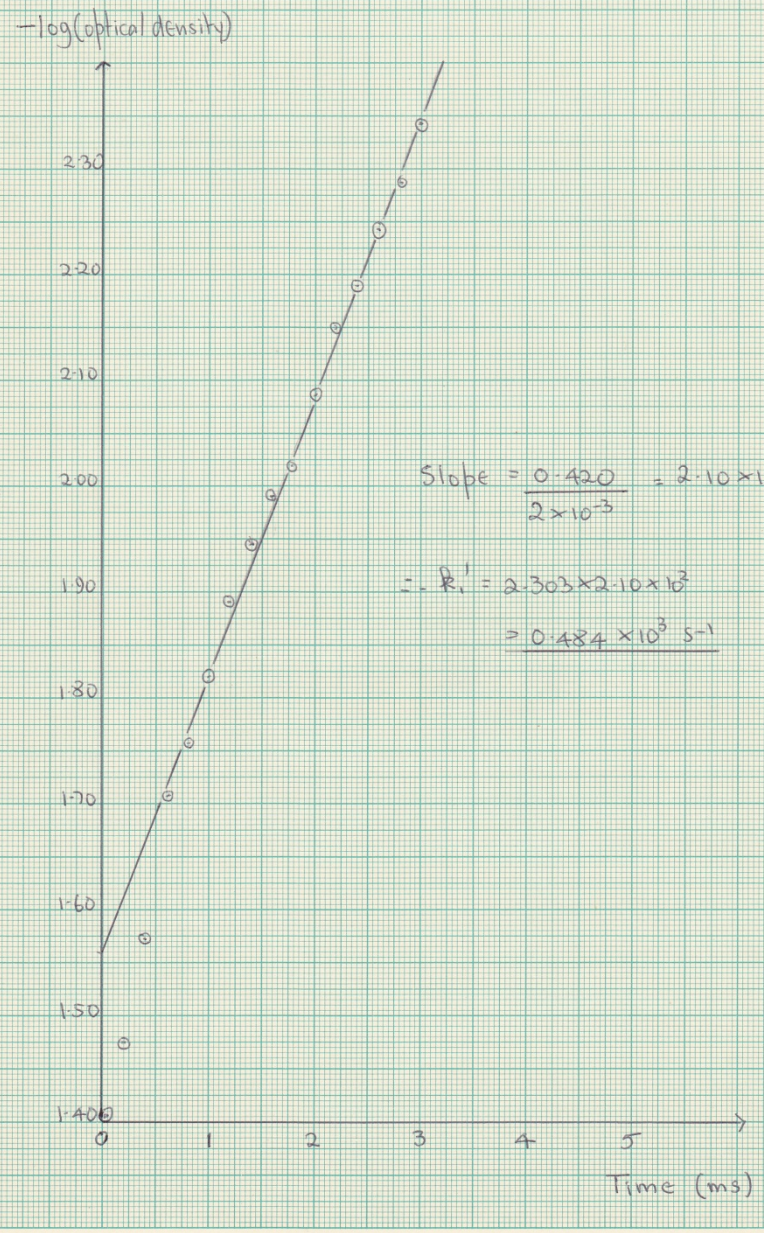

$$\text{Slope} = \frac{0.420}{2 \times 10^{-3}} = 2.10 \times 10^{2}$$

$$\therefore k_1' = 2.303 \times 2.10 \times 10^{2}$$

$$= 0.484 \times 10^{3}\ s^{-1}$$

Fig 3.13 First Order Decay Plot for a 1.5×10^{-3}M Ester + 2.5×10^{-4}M $CuSO_4$ solution in Methanol/Water

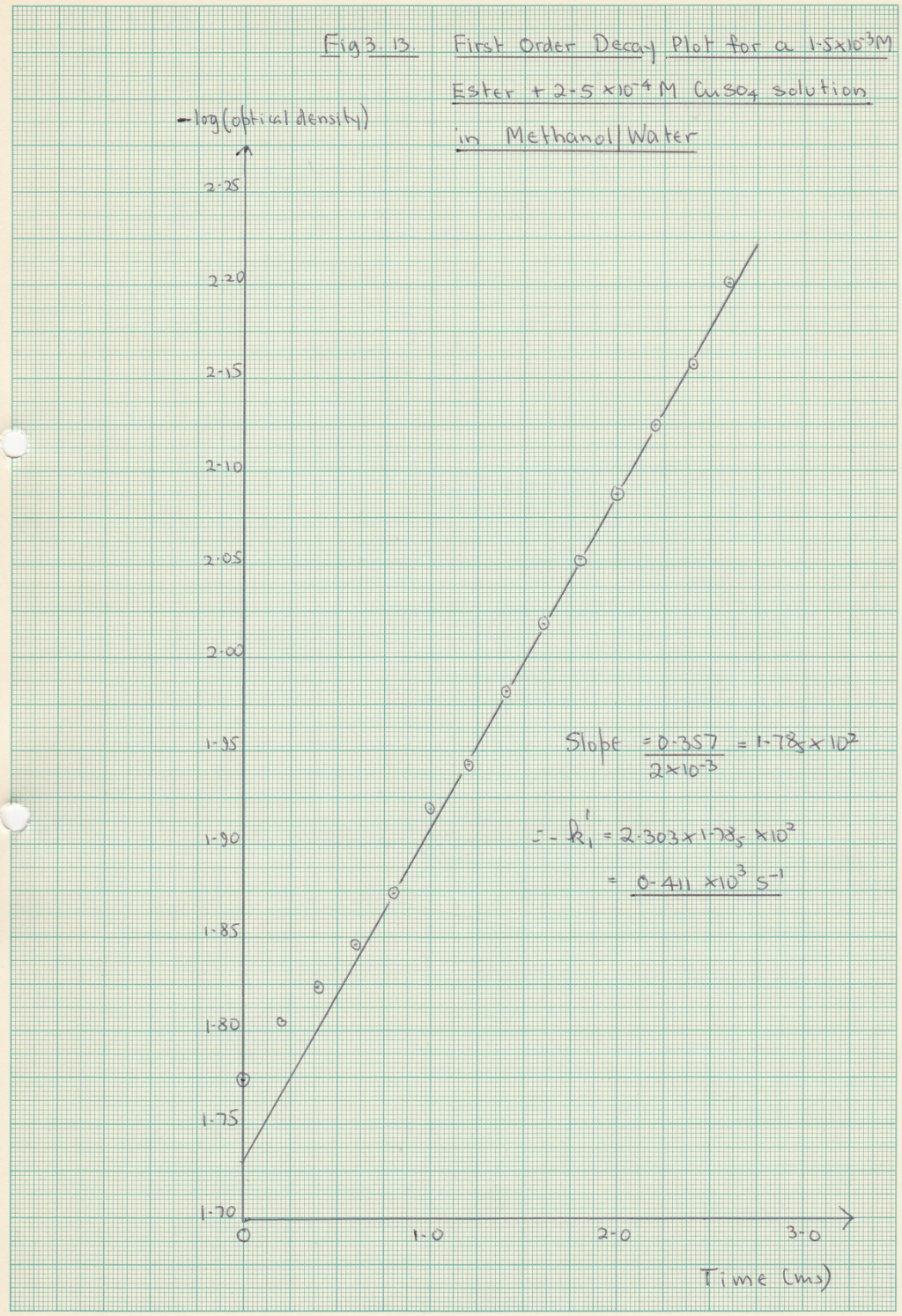

Slope $= \frac{0.357}{2 \times 10^{-3}} = 1.78_5 \times 10^2$

$\therefore -k_1' = 2.303 \times 1.78_5 \times 10^2$

$= 0.411 \times 10^3\ s^{-1}$

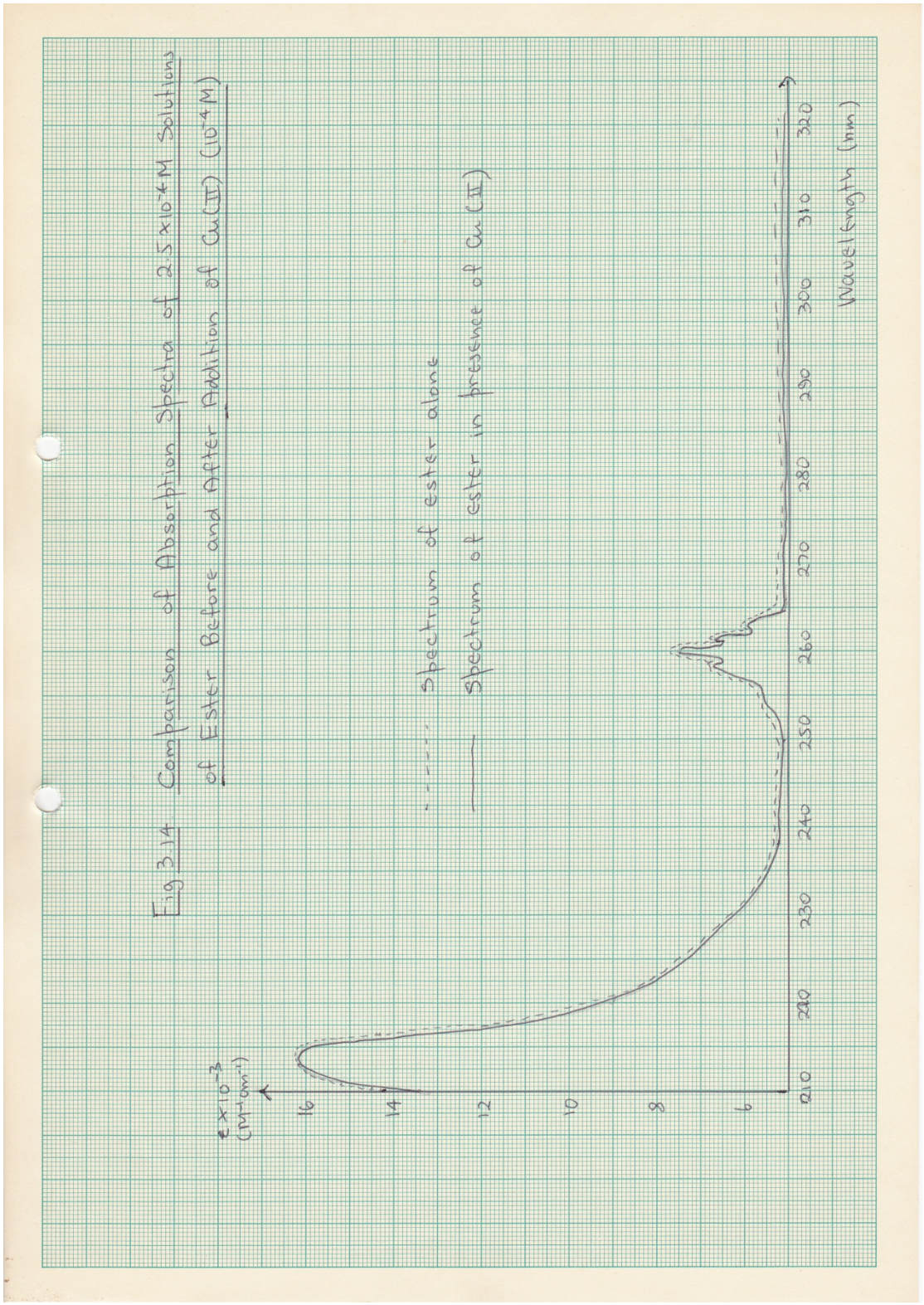
Fig 3.14 Comparison of Absorption Spectra of 2.5×10⁻⁴M Solutions of Ester Before and After Addition of Cu(II) (10⁻⁴M)
Spectrum of ester alone
Spectrum of ester in presence of Cu(II)
ε×10⁻³ (M⁻¹cm⁻¹)
16
14
12
10
8
6
210
220
230
240
250
260
270
280
290
300
310
320
Wavelength (nm)

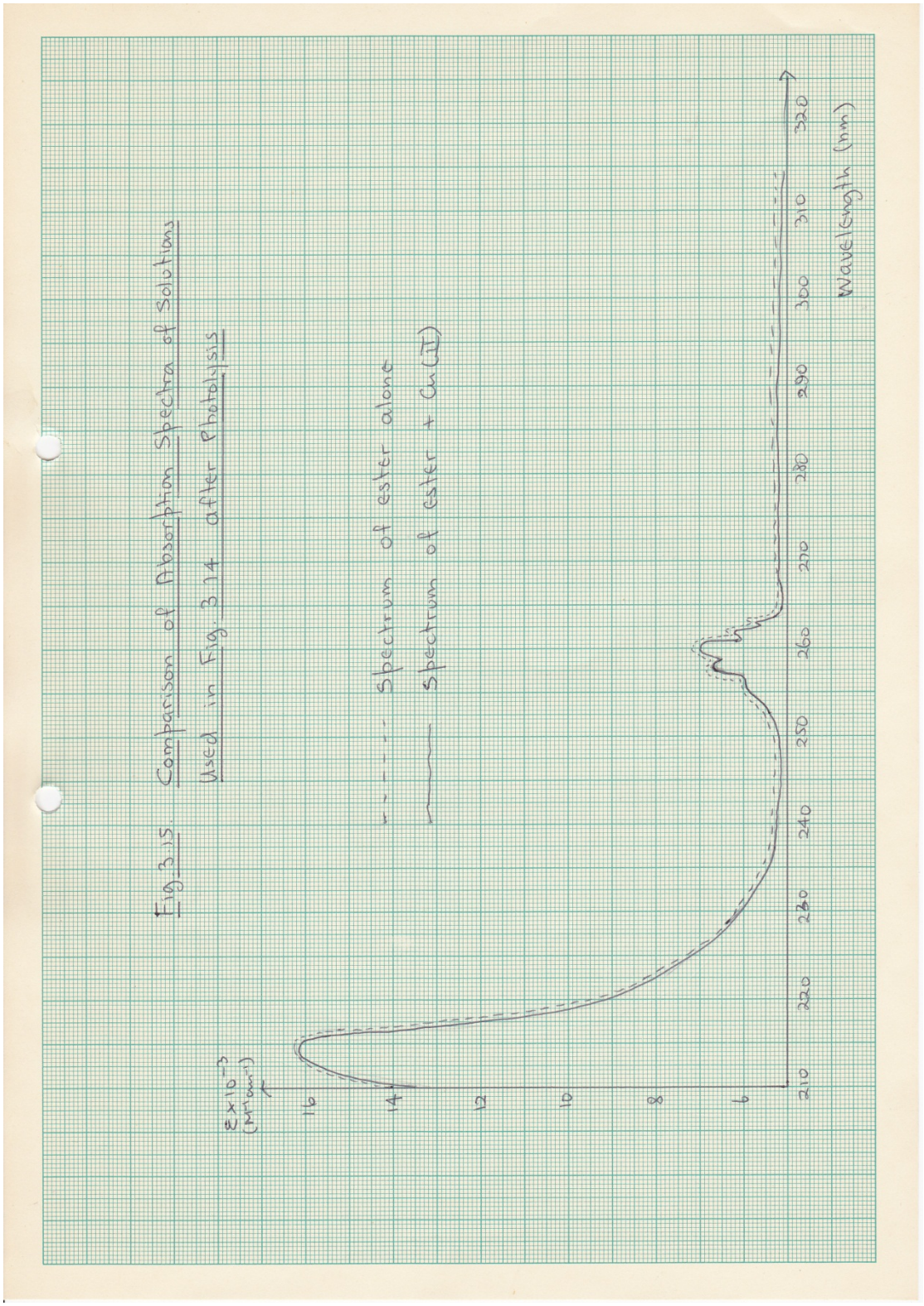
Fig. 3.15 Comparison of Absorption Spectra of Solutions Used in Fig. 3.14 after Photolysis
---- Spectrum of ester alone
——— Spectrum of ester + Cu(II)
ε x 10⁻³ (M⁻¹cm⁻¹)
16
14
12
10
8
6
210
220
230
240
250
260
270
280
290
300
310
320
Wavelength (nm)

Fig 3.16 Comparison of Absorption Spectra of Transients before and after Addition of Cu(II)

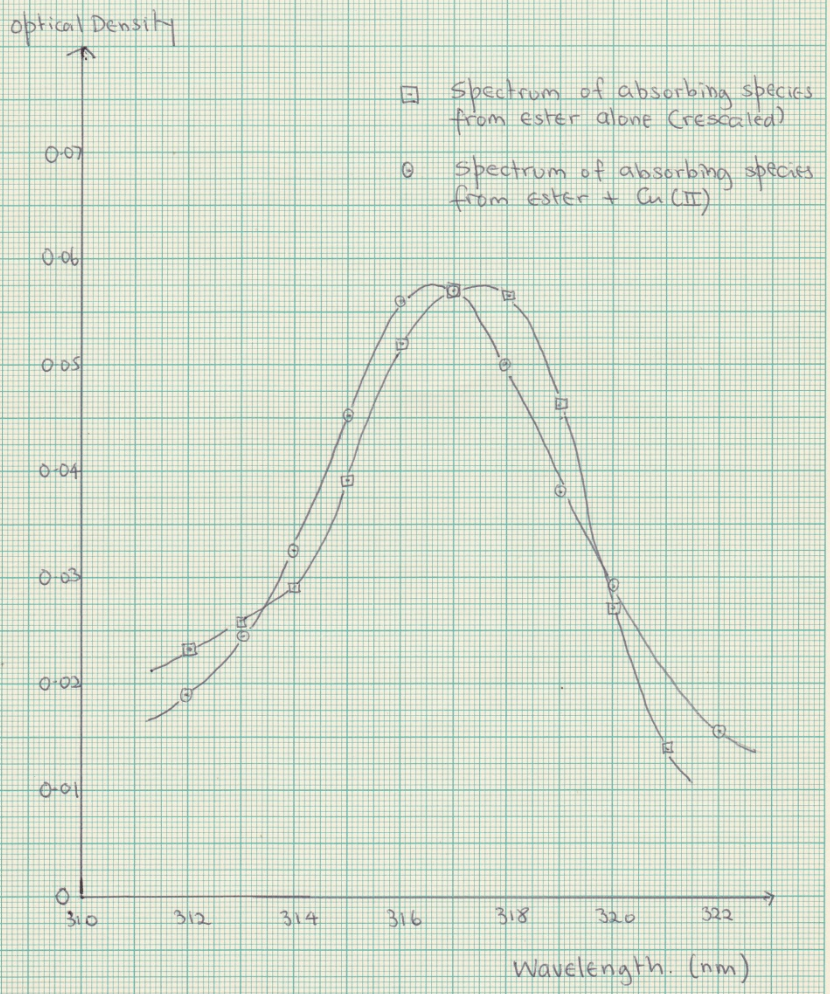

3.5 Discussion of Results and Suggestions for Future Work

The most obvious conclusion to be drawn from the results is that the overall situation is far more complicated than the expected simple second-order recombination of benzyl radicals. The nature of the first-order decay involving the benzyl radical was not clarified, but it is likely to be the result of a reaction with some impurity present (probably in the ester, since both methanol/water and cyclohexane give similar values for the first-order rate constant) which could not be removed by the purification methods attempted.

The analysis of the situation pertaining in the case of simultaneous first- and second-order decay described in Section 3.3.iv shows that, despite the kinetic complications of this first-order reaction, a value for k_2/ε should be obtainable if k_1 can be measured with sufficient accuracy. The graphical estimation of k_1 used here gives reasonable results, but the values could be checked in either of two more accurate ways. Firstly, values for k_1 and k_2 could be found by computer-fitting the data into the equation containing k_1 and k_2 for each determination, and this method would be expected to give far greater precision in the values of both k_1 and k_2. Secondly, it seems reasonable that the first-order reaction should have a greater activation energy than the second-order reaction (since the latter is a diffusion-controlled process, which is expected to have a very low activation energy – *ca.* 3.5 Kcal $mole^{-1}$) and so an increase in temperature should make the first-order reaction more dominant. Such a procedure would obviously be limited by the relatively low boiling-point of methanol (64°C), but a temperature increase of about 25° would be expected to increase the rate by a factor of approximately four, and would enable k_1 to be determined more accurately and more convincingly. A series of such determinations at different temperatures would enable values of k_2/ε to be extracted (as previously) as a function of temperature, and the value at 25°C could be obtained by extrapolation from a plot of $\log(k_2/\varepsilon)$ against T^{-1} which is expected to be linear over the temperature range considered. If such more accurate values of k_2/ε were obtained they would serve as a useful check on the literature values of the extinction coefficient at 318nm.

With regard to the possibility of studying cage recombination of the benzyl radicals as a function of temperature, it was decided, on the basis of the decay curves obtained with purified materials, that such an intended study would prove difficult. The amount of dibenzyl being produced was very small and consequently measurements of the dibenzyl optical densities would be susceptible to large errors, thus making any results obtained be necessarily of uncertain value.

In the case of the results in the presence of cupric ion, the nature of the decays obtained strongly suggests that something other than the decay of the benzyl radical is being followed. The effect of adding the salt should be to decrease the half-life of the decay, whereas an increase was observed in every case. Such an effect seems to be explicable in only two ways. The cupric salt could be functioning in some way so as to remove the impurity responsible for the first-order decay occurring in the absence of the cupric ion, and the decays observed are due to the subsequent reaction between Cu(II) and the free radical, but the independence of the first-order rate constant on cupric ion concentration appears to refute this. The second and most likely possibility has already been mentioned *viz.* that the observed decays are those of some cupric complex having a half-life of about 900μs. Formation of some species such as copper benzyl appears to be a reasonable suggestion, and the results can be rationalized on this basis if it is assumed that such a complex is formed very rapidly (within 100μs) after the initial photolysis of benzyl phenylacetate and that the complex has an absorption band around 318nm. The general impression obtained was that initial optical densities in the presence of the cupric ion were greater than those with the ester alone, which would suggest that the extinction coefficient of the complex is greater than that of the benzyl radical at 318nm *i.e.* it is greater than 10^4 $M^{-1}cm^{-1}$.

Such an explanation obviously requires further experimental investigation into the nature of the reaction. The kinetics of the reaction should be investigated over a wider range of concentrations (say 10^{-3} to 10^{-5} M) and the apparent independence of the first-order rate constant on cupric ion concentration confirmed or disproved. If this is found to be confirmed, it would remain to determine more satisfactorily the nature of the intermediate complex and to find its UV absorption spectrum more accurately in order to differentiate it sufficiently from that of the benzyl radical (this could probably be determined by using a flash spectrographic detection for each transient). The existence of copper alkyls has been proposed previously, and the suggested formation of copper benzyl is a consistent deduction from the data available at present,

but, as stated, the problem warrants further attention before becoming a completely acceptable explanation of the photolytic reaction.

SUMMARY

The Thesis involves a determination of the usefulness of a flash photolytic method of studying redox reactions of the benzyl radical (produced by photolysis of benzyl phenylacetate) with metal ions. Both recombination of benzyl radicals and reactions of the benzyl radical with Cu(II) are investigated. For the recombination reaction, complex kinetics are found, and it is suggested that the benzyl radical is undergoing simultaneous first- and second-order decay. Values of rate constants proposed are

$$k_1 = (0.78 \pm 0.06) \times 10^3\ s^{-1}$$

$$k_2/\varepsilon = (1.44 \pm 0.1) \times 10^5\ cm^{+1}s^{-1}$$

In the presence of the cupric ion, apparently anomalous kinetics are found and a rationalization is proposed on the basis of formation of copper benzyl whose half-life is determined to be approximately 900μs.

REFERENCES

(1) NOYES R.M., *Progress in Reaction Kinetics*, p. 129 (1961)

(2) NORTH A.M., *Collision Theory of Chemical Reactions in Liquids*, Methuen (1964)

(3) BENSON S.W., *Foundations of Chemical Kinetics*, McGraw-Hill (1960)

(4) DEBYE P., *Trans. Electrochem. Soc*., 82, 265 (1942)

(5) BACKSTROM H.L.J. & SANDROS K., *Acta Chem. Scand*., 14, 48 (1960)

(6) COLLINS F.C. & KIMBALL G.E., *J. Colloid Sci*., 4, 425 (1949)

(7) COLLINS F.C., *J. Colloid Sci*., 5, 499 (1950)

(8) FRANK J. & RABINOWITCH E., *Trans. Far. Soc*., 30, 120 (1934)

(9) NOYES R.M., *J. Chem. Phys*., 22, 1349 (1954)

(10) NOYES R.M., *J. Am. Chem. Soc*., 77, 2042 (1955)

(11) NOYES R.M., *J. Am. Chem. Soc*., 78, 5486 (1956)

(12) NOYES R.M., *J. Phys. Chem*., 65, 763 (1961)

(13) ROY J.C., WILLIAMS R.R. & HAMILL W.H., *J. Am. Chem. Soc*., 76, 3274 (1954)

(14) MONCHICK L., *J. Chem. Phys*., 24, 381 (1956)

(15) BASCO N. & SUART R.D., *Int. J. Chem. Kinet*., 2, 215 (1970)

(16) KOCHI J.K., *J. Am. Chem. Soc*., 92, 4395 (1970)

(17) BURKHART R.D., *J. Phys. Chem*., 73, 2703 (1969)

(18) CARLSSON D.J., INGOLD K.U. & BRAY L.C., *Int. J. Chem. Kinet*., 1, 315 (1969)

(19) UMANSKII V.M. & STEPUKHOVICH A.D., *Zh. Fiz. Khim*., 43, 2490 (1969)

(20) COME G.M., BARONNET F., MARTIN R. & NICLAUSE M., *C. R. Acad. Sci., Paris, Ser. C*, 267, 1192 (1968)

(21) STEPUKHOVICH A.D. & ULITSKII V.A., *Zh. Fiz. Khim*., 42, 1267 (1968)

(22) KONDRAT'EV V., *Kinet. Katal*., 8, 965 (1967)

(23) KOMINAR R.J., JACKO M.G. & PRICE S.J.W., *Can. J. Chem*., 45, 575 (1967)

(24) LYON R.K., *J. Am. Chem. Soc*., 86, 1907 (1964)

(25) ULITSKII V.A. & STEPUKHOVICH A.D., *Zh. Fiz. Khim*., 37, 689 (1963)

(26) MOSELEY J.C. & ROBB F., *Proc. Roy. Soc*., A243, 119 (1957)

(27) SHEPP A. & KUTSCHKE K.O., *J. Chem. Phys*., 26, 1020 (1957)

(28) SZWARC M., HERK L. & FELD M., *Int. Symp. Free Rads. 5th. Uppsala*, B.1 (1961)

(29) MATSUOKA M., DIXON P.S., STEFANI A.P. & SZWARC M., *Proc. Chem. Soc*., 304 (1962)

(30) GILLIS H.A., *J. Phys. Chem*., 71, 1089 (1967)

(31) VOGT T.C. & HAMILL W.H., *J. Phys. Chem*., 67, 292 (1963)

(32) LEBEDEV Ya. S., TSVETKOV Yu. D. & VOEVODSKII V.V., *Int. Symp. Free Rads. 5th. Uppsala* (1961)

(33) HERK L., FELD M. & SZWARC M., *J. Am. Chem. Soc*., 83, 2968 (1961)

(34) IMAI M. & TOYAMA O., *Bull. Chem. Soc. Japan*, 33, 652 (1960)

(35) HEILMANN W.J., REMBAUM A. & SZWARC M., *J. Chem. Soc*., 1127 (1957)

(36) SMID J. & SZWARC M., *J. Am. Chem. Soc*., 78, 3327 (1956)

(37) LEVY M. & SZWARC M., *J. Am. Chem. Soc*., 77, 1949 (1955)

(38) SOMER & MAIN, *J. Phys. Chem*., 72, 3856 (1968)

(39) WEINER S. & HAMMOND G.S*., J. Am. Chem. Soc*., 90, 1959 (1968)

(40) HAGEMANN R.J. & SCHARWZ H.A*., J. Phys. Chem*., 71, 2694 (1967)

(41) BURRELL E.J. & BHATTACHARYA P.K*., J. Phys. Chem*., 71, 774 (1967)

(42) BURKHART R.D., *J. Am. Chem. Soc*., 90, 273 (1968)

(43) CARLSSON D.J. & INGOLD K.U*., J. Am. Chem. Soc*., 90, 1055 (1968)

(44) FESSENDEN R.W., *J. Phys. Chem*., 68, 1508 (1964)

(45) TAUBE H., *Adv. in Inorg. Chem. & Radiochem*., p.1, (1959)

(46) HALPERN J., *Quart. Rev*., 15, 207 (1961)

(47) TAUBE H., *Adv. Chem. Ser. Am. Chem. Soc. Spec. Publn*., 49, 107 (1965)

(48) SUTIN N., *Ann. Rev. Nucl. Sci*., 12, 285 (1962)

(49) MARCUS R.A., *Ann. Rev. Phys. Chem*., 15, 155 (1964)

(50) STRANKS D.R. in LEWIS & WILKINS *Modern Co-ordn. Chem*. (1960)

(51) DIEBLER H. & SUTIN N., *J. Phys. Chem*., 68, 174 (1964)

(52) SUTIN N., *Ann. Rev. Phys. Chem*., 17, 119 (1966)

(53) MASSEY H.S.W. & BURHOP E.H.W., *Electronic Ionic Impact Phenomena,* O.U. Press (1952)

(54) MARCUS R.J., ZWOLINSKI B. & EYRING H., *J. Phys. Chem*., 58, 433 (1954)

(55) WEISS J., *Proc. Roy. Soc*., A222, 128 (1954)

(56) MARCUS R.A., *J. Phys. Chem*., 24, 970 (1956)

(57) MARCUS R.A., *J. Chem. Phys*., 24, 966, 979 (1956)

(58) MARCUS R.A., *J. Chem. Phys*., 26, 867 (1957)

(59) MARCUS R.A., *Disc. Far. Soc*., 29, 129 (1960)

(60) HUSH N.S., *Z. Electrochem*., 61, 734 (1957)

(61) HUSH N.S., *J. Chem. Phys*., 28, 962 (1958)

(62) HUSH N.S., *Trans. Far. Soc*., 57, 557 (1961)

(63) DE LA MARE H.E., KOCHI J.K. & RUST F.F., *J. Am. Chem. Soc*., 85, 1437 (1963)

(64) HAINES R.M. & WATERS W.A., *J. Chem. Soc*., 4255 (1955)

(65) COLLINSON E., DAINTON F.S., MILE B., TAZUKE S. & SMITH D.R., *Nature*, 198, 26 (1963)

(66) BAMFORD C.H., JENKINS A.D. & JOHNSTON R., *Proc. Roy. Soc*., A239, 214 (1957)

(67) KOCHI J.K. & SUBRAMANIAN R.V., *J. Am. Chem. Soc*., 87, 4855 (1965)

(68) PORTER G. & WRIGHT F.J., *Trans. Far. Soc*., 51, 1469 (1955)

(69) PORTER G. & STRACHAN E., *Specta. Acta*., 22, 803 (1966)

(70) PORTER G. & WINDSOR M.W., *Nature*, 180, 187 (1957)

(71) PORTER G. & SAVADATTI M.I., *Specta. Acta*., 12, 299 (1958)

(72) GRAJCAR L. & LEACH S., *Comptes Rendus*, 252, 1014 (1961)

(73) McCARTHY R.L. & MACLACHLAN A., *Trans. Far. Soc*., 56, 1187 (1960)

(74) HODGKIN J.E. & MEGARITY E.D., *J. Am. Chem. Soc*., 87, 5322 (1965)

(75) GALLIVAN J.B. & HAMILL W.H., *Trans. Far. Soc*., 61, 1960 (1965)

(76) BURK HART R.D., *J. Phys. Chem*., 73, 2703 (1969)

(77) TOPP M.R., Private Communication (1971)